Micro- and nanomechanical sensors for environmental, chemical, and biological detection

Philip S. Waggoner and Harold G. Craighead*

Received 15th May 2007, Accepted 27th June 2007
First published as an Advance Article on the web 25th July 2007
DOI: 10.1039/b707401h

Micro- and nanoelectromechanical systems, including cantilevers and other small scale structures, have been studied for sensor applications. Accurate sensing of gaseous or aqueous environments, chemical vapors, and biomolecules have been demonstrated using a variety of these devices that undergo static deflections or shifts in resonant frequency upon analyte binding. In particular, biological detection of viruses, antigens, DNA, and other proteins is of great interest. While the majority of currently used detection schemes are reliant on biomarkers, such as fluorescent labels, time, effort, and chemical activity could be saved by developing an ultrasensitive method of label-free mass detection. Micro- and nanoscale sensors have been effectively applied as label-free detectors. In the following, we review the technologies and recent developments in the field of micro- and nanoelectromechanical sensors with particular emphasis on their application as biological sensors and recent work towards integrating these sensors in microfluidic systems.

Introduction

Micro- and nanomechanical sensors

The development of atomic force microscopy (AFM) demonstrated the utility of a cantilevered sharp tip in mechanically probing a surface.[1] This tip is either scanned in contact with the surface, using cantilever deflection to map sample topography *via* the tip–sample interaction force, or it is resonantly excited slightly above the sample, monitoring changes in the resonant properties of the cantilever to probe the surface. Since then, the versatility of this technique has been demonstrated by the development of numerous new sensing modes, *e.g.* capacitance or magnetic-based AFM, as well as applications of cantilevers and similar micro- and nanoelectromechanical systems (MEMS and NEMS) as sensors.

Recently, micro- and nanometre scale cantilevers have been studied as sensors using physical principles that are similar to those found in atomic force microscopy. These cantilevers are generally operated in either the static deflection mode, where binding on one side of a cantilever causes unbalanced surface stress resulting in a measurable deflection up or down, or the dynamic, resonant mode, where binding on the cantilever increases mass and thus decreases the resonant frequency, much like quartz crystal microbalances. Cantilever-based devices have been demonstrated as highly versatile sensors using mechanical, optical, electrostatic, and electromagnetic methods for actuating or sensing cantilever motion in order to detect gases, chemicals, or biological entities.

The microfabricated devices can be made in different shapes and sizes and formed in arrays with large numbers of elements. With appropriate chemical functionalization they can be multiplexed for the detection of different chemical or biological entities. The size and flexibility of design suggests the possibility of incorporation in microfluidics and miniaturized lab-on-a-chip formats. The deflection mode sensors are a more mature technology and consist of various cantilever structures. Resonant mode devices are often cantilevers of the same type, but the oscillating elements can be made in a wider range of geometries. The dynamic mode devices are being explored in different configurations, including arrays of ultra-low mass resonators for detection of small bound mass.

Label-free biological detection

As biomedical research continues to find new proteins or chemical markers associated with a disease or condition, interest grows in detecting these markers as an alternative to symptomatic diagnosis. Ideally, one would be tested for these markers periodically, giving insight into the onset of disease. In addition, developing techniques that could detect sufficiently low quantities would lead to the ultimate in early detection of disease.[2] As a result, current research in this field is focused on maximizing sensitivity, reducing false positives and negatives, and creating highly-multiplexed systems for parallel detection of any number of biomolecules of interest. Effective systems would have far-reaching impact.

Many biological detection schemes involve labeling proteins chemically, typically with radioactive species, quantum dots, fluorescent markers, or enzymes.[3] These labeling schemes are then coupled with multiplexed bioassays, designed to detect an assortment of molecules. Typically, receptors with specific binding affinities to desired analytes are immobilized on a substrate, where the sample will be introduced. While these receptor–analyte systems are highly specific, interactions with other entities either by non-specific physisorption or cross-reactivity of the receptor with another biomolecule are still present. Non-specific binding is an important issue that affects all types of binding assays.

School of Applied and Engineering Physics, Cornell University, Ithaca, NY, 14853, USA. E-mail: hgc1@cornell.edu; Fax: +1 607-255-7658; Tel: +1 607-255-8707

Two examples of labeled detection include immunoassays, which use antibody receptors to bind their specific antigens in the sample solution, and protein microarrays,[4] used to detect protein binding to a wide variety of biological molecules. Detection is usually signaled in one of the following ways: studying the competitive binding of labeled and unlabeled analytes, using labeled molecules specific to immobilized analytes, forming a sandwich assay, or performing an enzyme-linked immunosorbent assay, or ELISA, where an enzyme-active substrate is added that changes color or fluoresces upon interaction with enzyme-linked analytes.[3] Some other examples of labeled biosensing include immunoprecipitation (IP) and yeast two-hybrid (YTH) systems.[4]

However, labeled detection is not ideal. Additional time and costs are needed in order to label the biomolecules. Often, labels are connected to antigens or antibodies in a random way, and, depending on the binding site, the labels could interfere with the function of the protein, reducing its chemical activity. Also, new labels and labeling techniques often must be developed to complement newly discovered proteins of interest.[5] In addition, as the size of the molecule relative to its label decreases, steric hindrance may become a problem in binding experiments with those molecules.[4] As the desired detection limits move into ng mL^{-1} and pg mL^{-1} concentrations, labeled detection becomes increasingly difficult, since common fluorescence techniques are not sensitive enough to distinguish very few fluoresced photons from the background.

This has encouraged the development of a wide variety of label-free detection systems that are equally or more sensitive than labeled detection techniques. Some of the most common include surface plasmon resonance (SPR), quartz crystal oscillators, calorimetry, nanowire and nanotube-based transistors, and micro- or nanoelectromechanical systems (MEMS or NEMS).[4–6] SPR is one of the more common techniques in label-free detection. It is a probe of the local index of refraction just outside a thin metallic film, typically functionalized gold, that is exposed to the sample solution. Changes in the excited plasmons in the metal are induced by analyte binding events that modify the local index of refraction. Quartz crystal oscillators are commonly used devices that can detect any adsorbed mass and have been used in both thin film deposition as well as biological detection. Upon applying an AC voltage to the crystal, mechanical resonance will occur; the resonant frequency is inversely proportional to the square root of the oscillator mass. Therefore, adsorbed mass effectively increases the sensor mass and decreases the resonant frequency accordingly. Field-effect transistor-based devices have also been made from nanowires or carbon nanotubes that show changes in conductance upon binding of charged molecules.[5] Quartz crystal microbalances (QCMs) have demonstrated sensitivities on the order of 1 ng cm^{-2} in fluid[7] or 10 pg cm^{-2} in vacuum,[8] while the best SPR systems have sensitivities of $\sim$100 pg cm^{-2}.[5]

MEMS and NEMS devices[9,10] create opportunities for novel, label-free detectors with high sensitivity and very high levels of multiplexing. Devices with small physical dimensions have exhibited excellent sensitivity and therefore potential for appropriately redundant and multiplexed biosensor arrays. For example, IBM has developed the "Millipede," a fully-integrated microcantilever array of 1024 devices that occupies a small area.[11] A portion of such an array of 50 μm long cantilevers is shown in Fig. 1, demonstrating both the uniformity and high density of these devices. One can imagine such an array with the ability to detect numerous analytes from a single sample. This level of bulk fabrication and sensor multiplexing is not easily accessible in other techniques like SPR or QCM. In addition, recent research has demonstrated detection of biological masses from picograms to attograms (10^{-12}–10^{-18} g) and sensitivity to concentrations on the order of nM or less.

Sensitivity and detectability

Mass sensitivity

Device sensitivity to small changes in mass is one type of sensitivity that is intuitively comparable to macroscale measurements. It is the natural figure of merit when detecting single small entities such as bacteria, viruses, nanoparticles, or individual molecules. Sensors with a very high absolute mass sensitivity could permit discrete sensing and enumeration of analytes. Resonant MEMS and NEMS devices actuated in vacuum have demonstrated mass sensitivity, measuring mass changes in the order of attograms or less.[12–15]

Sensors that work on larger scales typically measure changes in mass uniformly distributed over the sensor. As a result, sensitivities for quartz crystal microbalance and surface plasmon resonance techniques are often discussed in terms of mass per unit area. While this value can be translated into a value for total mass measured, the size of these devices restricts absolute mass sensitivity to the range of nanograms to picograms.

Chemical concentration sensitivity

For many applications the figure of merit of a sensor system is the detectable concentration of a chemical of interest in a medium that contains mixtures of other compounds often at much higher concentrations. In these cases, the chemical specificity and affinity of the chemical binding layer are the

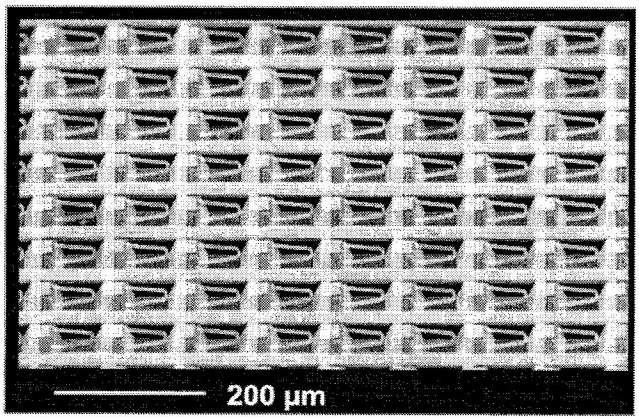

Fig. 1 Image of several cantilevers in a "Millipede" cantilever array, which contains an array of 32 × 32 fully integrated devices. Each cantilever is 50 μm in length. Image courtesy of W. P. King, reprinted from ref. 11.

critical and usually limiting features of a sensor. This is true for a NEMS or MEMS based sensor as it is for all other forms of sensors based on chemical binding mechanisms. The fluid dynamics and the kinetics of analyte binding and diffusion and transport to the receptor layer on the devices are also important. In addressing these issues, MEMS or NEMS devices may permit use of protocols that interface well to microfluidics and chip-based technologies, but they face the same chemical issues as sensors based on other binding transduction methods. Ultimately, the sensitivity of a technique is a function of more than just the physical limits of the sensor itself.

For medical diagnostic devices, the sensitivity to a low concentration of a disease-marker compound in a body fluid is the important parameter. For example, prostate specific antigen (PSA) is currently used as a biomarker for prostate cancer at concentrations in the range of 0.1 to 10 ng mL^{-1}. In other systems, sensitivity in the order of pM or fM may be desirable. However, these low concentration target compounds are in serum or other body fluids that have other constituents at much higher concentrations. These ubiquitous biomolecules can non-specifically bind to receptor molecules or device surfaces and reduce the sensitivity of the system, if not causing false positives or negatives. Therefore, blocking chemistries and other measures taken to reduce non-specific binding also play a significant role in determining the overall sensitivity of a sensor system.

The planar processing techniques used to create MEMS and NEMS sensors allow flexibility in the sensor system architecture in order to optimize the mass transport and fluid flow for a given sensor requirement. For example the size and number of devices can be chosen based on the sample volume of a lab-on-a-chip system. Arrays of small devices can be particularly advantageous in optimizing the sensitivity of the individual elements, increasing the sampling area with large numbers of devices and arranging the spacing and functionalization for the most efficient flow or diffusion-based delivery of analyte to the surface. Theoretical modeling of nanoscale sensors operating in fluid have demonstrated that using arrays of devices in a constrained volume can improve the overall sensor response in the limit of dilute analytes.[16] These improvements are dependent on the fill fraction of the sensors on the surface; the spacing can be optimized to the diffusion length of the analyte, such that the fluid volume sampled by each sensor does not overlap with that of its neighbors. Recent work has demonstrated the fabrication of nanomechanical resonators within microfluidic channels at a high density.[17]

In general, the sensor system performance is a function of numerous factors including chemical characteristics, fluid sampling, detection sensitivity and time requirements. NEMS and MEMS sensors should be considered as a flexible part of a lab-on-a-chip system but the physical properties of the mechanical elements are only one feature of the complete system.

Sensor fabrication and differentiation

Fabrication techniques

Typically, fabrication of MEMS and NEMS sensors takes advantage of one of two common MEMS photolithography processes—bulk or surface micromachining; simplified schematics of the two techniques as applied to cantilevers are shown in Fig. 2(a) and (b), respectively. The key difference between these techniques is the sacrificial layer which, when removed, releases the devices from the substrate. In bulk micromachining, the bulk silicon wafer is used as the sacrificial layer. The device layer, such as silicon nitride, is grown directly on a wafer that has been oxidized on the bottom. This oxide is then patterned in order to mask an anisotropic silicon etch, like KOH or tetramethyl ammonium hydroxide (TMAH), that will undercut the devices and release them from the substrate, allowing them to bend or resonate. In surface micromachining, there is no back side processing, and the silicon wafer is left intact. A sacrificial oxide layer is first grown on a silicon wafer, followed by deposition of the device layer. Standard photolithography techniques are used to mask anisotropic etching of the device layer, typically performed using a dry reactive ion etch process. Hydrofluoric acid is then used to etch the sacrificial oxide layer and release the structures, suspending them above the silicon substrate.

While surface micromachining requires one less photolithography step, the close proximity of the devices to the silicon wafer may present a problem in some applications. If the sacrificial layer is not thick enough for particularly long or flexible devices, stiction may occur if the suspended device layer comes in contact with the surface—this typically permanent problem makes the devices unusable. Stiction can be avoided by using bulk micromachining, which also opens up the possibility of addressing both sides of the cantilever. Critical point drying can also be used to prevent stiction, as it is often caused by capillary forces which come about during drying of released devices. Recent work has shown that

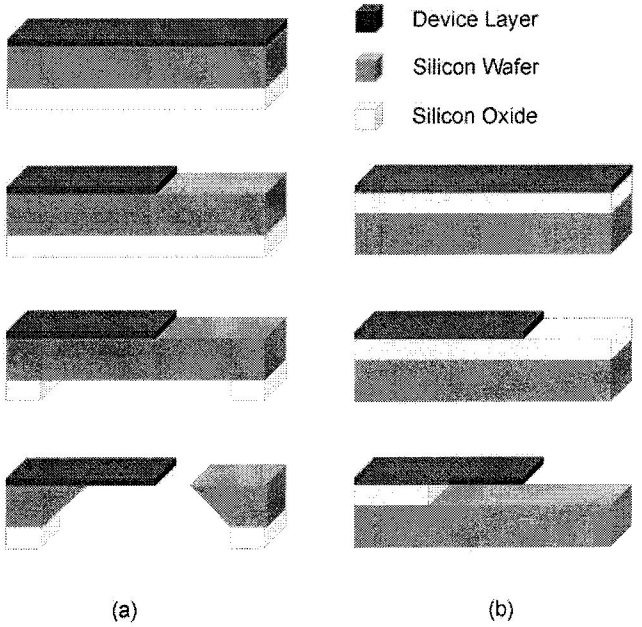

Fig. 2 Basic depiction of (a) bulk and (b) surface micromachining processing steps leading to suspended devices. In bulk micromachining the wafer acts as the sacrificial layer that is removed to release the devices, while in surface micromachining the sacrificial layer, typically silicon oxide, is fabricated directly on the wafer.

antibody activity is not affected significantly by critical point drying prior to introduction of the sample, suggesting that critical point drying may also be a good option for drying biosensors that are prone to stiction.[18]

Fabrication of NEMS devices, however, can require non-standard techniques in order to define structures on the nanoscale. Silicon-on-insulator wafers can be used to fabricate single crystal devices with nanoscale thicknesses, and the built-in, insulating oxide layer functions as a sacrificial layer to allow release of the devices. Electron beam lithography has been used with silicon-on-insulator wafers to define suspended nanowires that are 50 nm thick, 120 nm wide, and 7 to 13 μm long.[19] Recently, long suspended nanostrings with widths on the order of a few hundred nanometres have been fabricated using a non-lithographic technique, where poly(methyl methacrylate) (PMMA) nanofibers are deposited *via* electrospinning and used to define the nanoscale structures, shown in Fig. 3.[20,21]

Device functionalization

The surface chemistries used in functionalization of MEMS and NEMS sensors give the devices their capability for sensing. Coated with receptor layers specific to a particular analyte, sensor signals can then be attributed to analyte detection. To detect chemicals or vapors present in air, cantilevers are typically functionalized with a film that either specifically adsorbs the analyte or shows a higher affinity response compared to other films. Gold coated microcantilevers have been used to detect mercury vapor, which adsorbs to gold with significant affinity.[22] Water vapor sensors have been demonstrated with phosphoric acid and gelatin-coated cantilevers.[23] Other examples include polymer films that adsorb volatile organic compounds[24] or chemicals relevant to artificial nose technology.[25]

Mechanical biosensors use the same binding chemistries as conventional assay techniques. Immunoassays can be performed by coating devices with an antibody and detecting its antigen from solution, or *vice versa*. Tethering single-stranded DNA (ssDNA) to the cantilever can serve as a sensor for hybridization with the complementary strand of DNA.[26] Another method using enzymes has demonstrated glucose detection with glucose oxidase-coated cantilevers.[27] Liposomes have also been sensed, using capture layers that specifically bind to chemical groups on the liposome surface.[28] A newer technique of surface linking chemistry for MEMS and NEMS sensors uses aptamers, nucleic acids that behave like antibodies, for binding a specific compound.[29] A thorough review of molecular recognition and detection chemistries for biological sensors that are either in use or development has been presented by Iqbal *et al.*[30]

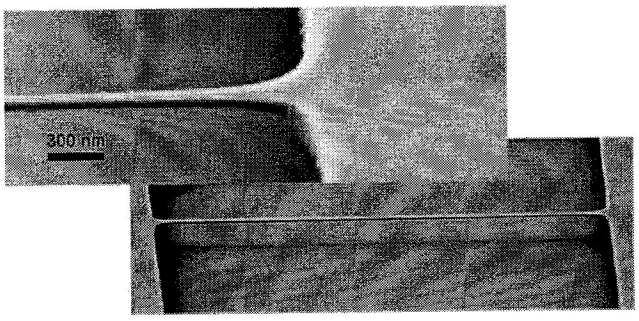

Fig. 3 SEM micrograph of a 15 μm long, doubly-clamped nanomechanical resonator fabricated non-lithographically. Electrospun fibers are used as an etching mask in order to define the nanostring resonators. Reprinted with permission from ref. 21. Copyright 2006, American Institute of Physics.

There is, however, a fair amount of complexity introduced by these linking chemistries. If special care is not taken, receptor molecules will nonspecifically adsorb on the sensor surface and potentially block specific binding sites on a portion of the molecules and in turn reduce device sensitivity. Neutron reflectivity experiments have shown that, without using linking chemistries, antibodies will adsorb flat onto SiO_2 surfaces, rather than the fully functional upright configuration, which degrades the antigen binding capacity of the antibodies.[31] Also, at sufficiently high surface densities, conformational changes or steric hindrance effects from neighboring antibodies could reduce affinity for antigen binding.[32] Methods using amine reactive linkage to antibodies, for instance, may result in a random orientation of antibodies as they possess many addressable amine groups. In addition, tethering proteins to surfaces can detrimentally change their conformation or even denature them, depending on the type of link and where on the protein it is made.[33] Protein G has been used as a surface treatment that results in a more oriented attachment of antibodies. Other processes use the avidin–biotin linking chemistry, but that requires biotinylation of the receptor molecule. This process often results in attachment of several biotin molecules, subjecting the receptor layer to random attachment to the avidin-coated surface and therefore degradation of device sensitivity. These and other immobilization methods are quantitatively compared in ref. 34. One common method of oriented immobilization uses receptor molecules that have been chemically modified with a thiol group that selectively binds to thin films of gold on the sensor. Another recent study has demonstrated improved biosensor sensitivity using antibodies linked to the surface by a ligand that is specifically attached to the antibody at the junction of the Fab and Fc regions.[35]

Single-chain Fv (scFv) or Fab antibody fragments offer potential solutions to many of these issues. By extracting the antigen-specific parts of the antibodies and using thiol groups to immobilize them on gold surfaces, the density of antigen binding sites is increased due to the smaller size of the fragments as well as their upright arrangement. This technique has led to significantly improved sensitivities for microcantilevers,[36] SPR,[37] and protein microarrays.[38]

Besides increasing the affinity of biosensor receptor molecules, there are other challenges in surface chemistry. Microcantilevers have been demonstrated as pH sensors using a variety of surfaces, including gold coated silicon and silicon nitride, aminosilane monolayers, and thiol monolayers on gold.[39] While these are useful results, they also warn of background pH effects in all MEMS and NEMS biosensors since a majority of applications uses one of these surface chemistries in some form. Another daunting problem for biosensors is non-specific binding. This is often addressed by

implementing a blocking chemistry. While many proteins or chemicals are used as blocking agents, such as bovine serum albumin, casein, or polyethylene glycol (PEG), it is not obvious which technique is most effective for particular surface chemistries. Careful planning of experimental procedure and using appropriate controls to measure a background for subtraction are often necessary to avoid these effects and produce biosensors with meaningful results. Non-specific binding remains a significant limit on ultimate detection sensitivity.

Deflection-based sensors

For sensor systems where analyte binding induces surface stress, flexible cantilevers functionalized on one side are used to transduce that stress into a measurable deflection. The operating principles and physics behind deflection-based MEMS and NEMS sensors will be briefly discussed in the following. In addition, some of the most recent developments in this field will be highlighted. More comprehensive reviews that focus on deflection-based cantilever sensors have been presented by Lavrik *et al.*,[40] Ziegler,[41] and Carrascosa *et al.*[42]

Principles of operation

Deflection-based MEMS and NEMS sensors of all types operate on the physical principles described by G. G. Stoney while studying tension and delamination of thin metal films in 1909.[43] Observing that when metals are deposited under tension they can sometimes bend the substrate, he developed what is now known as Stoney's formula,

$$R = \frac{Et^2}{6\sigma(1-\upsilon)} \quad (1)$$

where R is the radius of curvature, E is the Young's modulus, t is the thickness of the substrate, σ is the surface stress, and ν is the Poisson's ratio of the substrate. If this concept is applied to a microcantilever experiencing a surface stress, a decreasing radius of curvature will result in increased deflection at the free end of the cantilever. Therefore, if analyte binding to a particular surface causes a surface stress, cantilevers with that same surface will bend up or down, signifying detection. By far, the most common way to measure this deflection is to use optical reflection; a laser is focused on the cantilever and reflected onto a position sensitive detector. Cantilever deflection is then determined from the varying detector signal due to motion of the reflected laser beam.

Silicon or silicon nitride cantilevers are generally used because of the widespread use of silicon in microelectronics and also the compatibility and availability of fabrication methods for cantilevers and integrated circuitry. However, upon inspection of eqn (1), it is evident that the cantilever radius of curvature can be further decreased if a less stiff material were used. Calleja *et al.*[44] fabricated cantilevered structures from SU-8, a polymer with a Young's modulus 50 times smaller than that of silicon or silicon nitride. These polymer cantilevers show superior stability compared to gold-coated silicon or silicon nitride cantilevers. The lack of a bilayer significantly decreases thermal deflection noise, and, in contrast to silicon based devices, the SU-8 shows minimal response to changes in pH from 2 to 11. This is accomplished by using a thin fluorocarbon film to block one side of the devices rather than using a large gold layer to functionalize only one side. Using biotin and streptavidin as the receptor and analyte, respectively, they observe a 600 nm deflection for 200 μm long cantilevers, which is roughly an order of magnitude greater than sensor responses typical of silicon cantilevers with comparable lengths. While these cantilevers were probed using optical deflection, SU-8 cantilevers embedded with a carbon-based piezoresistor have also been demonstrated for electronic deflection measurement.[45] Ransley *et al.* tested the feasibility of using the gold-thiol chemistry with SU-8 polymer cantilever arrays.[46] Compared to results for SU-8 cantilevers without gold, the bilayer structure shows a very large deflection response of the cantilevers to a temperature increase of only one degree. Cantilevers fabricated from silicon oxide have also been shown to exhibit an order of magnitude increase in deflection response to identical chemical treatment when compared to silicon cantilevers.[47]

Adsorption-induced bending of cantilevers was seen initially in the formation of alkanethiol self-assembled monolayers (SAM) on a gold coated cantilever.[48] Soon after, this concept was applied to detect DNA hybridization using ssDNA molecules as immobilized receptors on a microcantilever.[26] This technique was demonstrated to be sensitive to single base pair mismatches, since cantilevers with such mismatched receptor molecules did not support hybridization, allowing them to be used as a reference cantilever for detection of the complementary DNA strand. Prostate-specific antigen was detected at low concentrations using immunoassay techniques on microcantilevers.[49]

The origin of the surface stresses that give rise to nanomechanical bending in cantilevers has been much debated. Cantilever bending was shown to increase with alkanethiol molecule length and concentration, suggesting electrostatic repulsion from the dipole-like molecules as dipole moment increases with chain length.[48] Steric and electrostatic repulsion were also suggested for DNA biosensors, since hybridization doubles the number of negatively-charged molecules on the surface.[26] These results were disputed by Wu *et al.*,[50] who observed a relief in the stressed cantilever beams upon hybridization of ssDNA receptors rather than increased downward bending as previously seen. They suggest that, although electrostatic and steric repulsion are present, configurational entropy can supersede these forces and create unexpected cantilever bending depending on the ionic concentrations, which can change molecular packing densities *via* charge shielding. In this way, hybridization into rod-like helices reduces the configurational entropy and could induce upward bending as a result of relieved stress. However, McKendry *et al.*[51] used Langmuir adsorption kinetics to determine the effect of ion concentration on ssDNA binding densities, and claimed that there was a minimal change in device saturation, pointing to steric repulsion.

In water, negatively-charged DNA develops a network of hydrogen-bonded water surrounding the molecule; perturbations of this network result in so-called hydration forces. These are suggested by Hagan *et al.* to account for the

steric-repulsion type dependence of cantilever bending on surface density.[52] They also find that in cases of weak interaction between DNA molecules, *i.e.* when hydration forces are not present, that repulsive osmotic pressure due to the ionic concentration dominates electrostatic forces by an order of magnitude.

These arguments concerning the bending dependence on surface density and its mechanisms were unified in a comprehensive study.[53] The ssDNA grafting density was measured as a function of immobilizing salt concentration, and two concentration-dependent regimes were observed. This revealed that at high salt concentrations the surface density is saturated, agreeing with the studies by McKendry *et al.*[51] Towards lower salt concentrations, the grafting density becomes strongly dependent on the salt concentration, pointing to the emergence of osmotic pressure.[52] Stachowiak *et al.* conclude that osmotic forces dominate at low salt concentrations, until the grafting density allowed by the salt becomes large enough that hydration forces begin to dominate, after which further increasing salt concentrations has no effect.[53] However, if another cantilever system with a different stiffness is used, the regimes of interaction may be completely different and significantly change the physics of the biosensor.[52]

Recent deflection-based sensors

A variety of gaseous and liquid-based chemical sensors have been developed to detect changes in environmental conditions or particular chemical vapors. Ji *et al.* observed the bending responses of several cantilever material and coating combinations in solution as a function of pH.[39] Sensitivity to pH values ranging from 2 to 12 was demonstrated, while not all material combinations were sensitive across that entire pH range. In another example of pH detection, PMMA-coated silicon cantilevers demonstrated high sensitivity, but only on the very limited range of pH values from about 6 to 7.[54] Cantilevers functionalized with a variety of polymer coatings have been studied as an artificial nose, demonstrating the ability to detect, in the gas phase, a number of alcohols, solvents, and natural flavors.[25] An image of the array of cantilevers used in this study is shown in Fig. 4; the 500 μm long cantilevers are representative of the size of many devices used in deflection-based sensing. Alkane-thiol self-assembled monolayers were recently used to detect toluene and water vapor with gold-coated silicon nitride cantilevers with considerable sensitivity at low vapor concentrations.[55] Microscale sensors responsive to all concentrations of carbon dioxide have been demonstrated, using a polycarbonate film as the active layer specific to CO_2.[56] Trinitrotoluene vapors have been detected using silicon oxide cantilevers coated with a thiol-based self assembled monolayer to which this explosive vapor adsorbs, demonstrated by detection at concentrations as low as 120 ppt.[57] In addition, mercury vapor adsorption to a gold film deposited on a cantilever produces significant surface stress and has been used in deflection-based micromechanical sensors.[22]

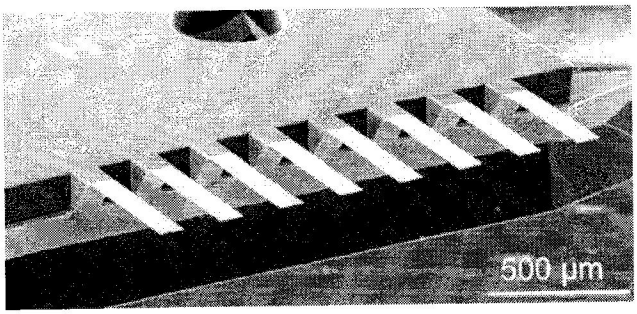

Fig. 4 Array of eight cantilevers used as deflection sensors for several chemical solvent vapors. The cantilevers, measuring 500 × 100 × 1 μm (length × width × thickness), are each coated with a different polymer in order to define a particular set of responses based on how each polymer responds to a given analyte. This figure is reprinted with permission from ref. 25. Copyright Elsevier, 2000.

Recently, static mode cantilever biosensors have demonstrated detection of several different analytes with both traditional and novel sensor designs. *Salmonella* bacteria strains have been detected using cantilevers functionalized with antibodies to the bacteria; a deflection was detected with as few as 25 bacteria attached to the device.[58] Cantilevers coated with a specific layer of short peptide chains were used to detect a concentration of roughly 10^8 *Bacillus subtilis* spores per mL due to static deflection of the device.[59] Creatin kinase and myoglobin were detected simultaneously within a liquid cell, at moderate concentrations of about 20 μg mL^{-1}.[60] Sensors for DNA transcription factors have also been constructed, using microcantilevers functionalized with double-stranded DNA.[61] Single-chain Fv antibody fragments were used in a cantilever array to detect engineered peptide antigens.[36] A unique method of surface chemistry using calixarene-derived Calixcrown linkers was used to sense the cancer biomarkers C-reactive protein and PSA at concentrations of 10 to 100 ng mL^{-1}.[62] Taq DNA polymerase has been sensed using aptamer-functionalized cantilevers.[29] These particular cantilevers are unique in that they are paired with a reference cantilever but only require a single laser beam to probe the relative deflection using a diffraction-based technique. Single-stranded DNA molecules with single base pair mismatches have been detected using piezoresistive cantilevers.[63] Specialized oligomers designed to bind to two different surface receptor molecules were detected at concentrations down to 10 nM. Concentrations of biotin as low as 100 pg mL^{-1} have been detected using a silicon cantilever that has a built-in metal-oxide semiconductor field effect transistor (MOSFET) at the base of the sensor.[64] Since the conductivity of silicon is strain dependent, deflections of the cantilever are read out as changes in the source to drain current of the transistor.

Conformational change has recently been presented as a new mechanism causing cantilever deflection. The stimuli responsible for inducing the conformational change are therefore available to be sensed by cantilevers functionalized with these biomolecules. Specialized DNA molecules have been shown to reversibly change from a folded, 4-stranded conformation into an elongated, duplex formation depending on the pH of the solution.[65] Other examples include conformational changes in human estrogen receptors with or without estradiol[66] and the membrane protein bacteriorhodopsin.[67]

Cantilevered, deflection-based MEMS sensors have shown potential for widespread use as biological sensors. A summary of these sensors and their respective materials systems and sensitivities are shown in Table 1. These devices are versatile in that they can be operated in air or transparent liquid, allowing real-time analysis, provided that there are no turbulences or significant fluctuations in temperature or the dielectric constant of the liquid. Static deflection methods also use reference cantilevers to subtract background and improve detection limits.

Some inherent limits to these devices are the need for one-sided functionalization, which almost always involves a gold/cantilever bilayer structure in order to utilize the gold–thiol linking chemistry. Despite the strong affinity of this binding relationship, the gold-device layer structure can increase background noise, since the bilayer structure is sensitive to temperature fluctuations as well as other environmental conditions to which the surfaces respond differently. Also, since cantilever tip deflection for a constant radius of curvature is proportional to the square of the cantilever length,[48] longer cantilevers are necessary for improved signals. As the lengths of these devices increase, they tend to require bulk micromachining techniques in order to overcome the increased risk of stiction during fabrication and operation. This keeps deflecting sensors from being easily integrated in microfluidics, requiring a fluid cell or additional encapsulation techniques.

Another limit to this technique of stress detection is that it is limited to the near monolayer regime. Single molecule adsorption can not generate a measurable deflection in a realistic device; for example, the lower limit for detection of DNA hybridization using deflecting cantilevers was found to be $\sim 2 \times 10^{10}$ hybridized molecules per mm^2.[51] It was also seen in mercury vapor detectors that if the gold film to which the mercury adsorbed was incomplete and in the form of isolated islands, the surface stress-related effects were absent, showing that a more complete receptor layer is needed in order to collectively achieve measurable deflections *via* surface stress.[22]

Resonant MEMS and NEMS sensors

Resonant micro- and nanoscale sensors consist of cantilevers operated in the dynamic mode as well as any other devices that can be excited at a stable resonant frequency. Recent work has demonstrated that these devices are now capable of measuring masses on the order of attograms.[12–15]

Resonating MEMS sensors have been used for some time, as mechanical sensors of force, flow, pressure, and acceleration[68] or as chemical sensors, while their application to biology is a more recent development. Despite the more common use of deflection-based cantilevers as biosensors due to their ability to function in fluid environments, resonant devices have shown superior ability to measure extremely small masses, and recent work has demonstrated new possibilities for improving device sensitivities and operating resonant sensors in fluid with enhanced mass resolution.

Resonance-based device principles

Resonant mechanical devices are commonly modeled as harmonic oscillators with a resonant frequency, f_0, given by

$$f_0 = \frac{1}{2\pi}\sqrt{\frac{k}{m}} \tag{2}$$

where k is the spring constant and m is the mass of the oscillator. If some mass, Δm, is added to the device and is small compared to the oscillator mass, the change in frequency, $\Delta f = f - f_0$, due to that mass can be approximated to the first order by

$$\Delta f = -\frac{1}{2}\frac{\Delta m}{m} f_0 \tag{3}$$

For a resonant sensor functionalized to specifically bind a particular analyte, knowing the resonant frequency before and after the binding step allows one to associate the change in frequency with an amount of bound analyte. Fig. 5 shows superimposed resonance curves taken during device functionalization for a baculovirus sensor.[69] The negative shifts in resonant frequency after formation of the antibody receptor layer and binding of the viruses result from increases in the resonator mass and can be used to determine the mass of the adsorbed molecules.

The most common type of resonant MEMS or NEMS sensor is the cantilever. The resonant frequency of the fundamental, out-of-plane mode has been calculated[70] to be

$$f_0 = \frac{3.515}{2\pi}\frac{1}{l^2}\sqrt{\frac{EI}{\rho A}} \tag{4}$$

where l is the cantilever length, I is the moment of inertia, ρ is density, and A is the cross-sectional area of the beam. Using

Table 1 Examples of deflection-based cantilever biosensor applications

Analyte	Minimum detected	Device layer	Detection method	Reference
Biotin	100 fg mL^{-1} (0.4 Nm)	Silicon	MOSFET	64
PSA	0.2 ng mL^{-1}	Silicon nitride	Optical reflection	49
Taq DNA polymerase	4.7 ng mL^{-1}	Silicon	Diffraction	29
PSA	$\sim$10 ng mL^{-1}	Silicon nitride	Piezoresistance	62
GCN4 antigenic peptide	20 ng mL^{-1}	Silicon	Optical reflection	36
myoglobin	20 μg mL^{-1}	Silicon	Optical reflection	60
DNA	10 nM	Silicon	Optical reflection	26
DNA	10 nM	Silicon nitride	Piezoresistance	63
DNA	75 nM	Silicon	Optical reflection	51
DNA transcription factors SP1 & NF-κB	$\sim$100 nM	Silicon	Optical reflection	61
Glucose	$\sim$10 mM	Silicon	Optical reflection	27

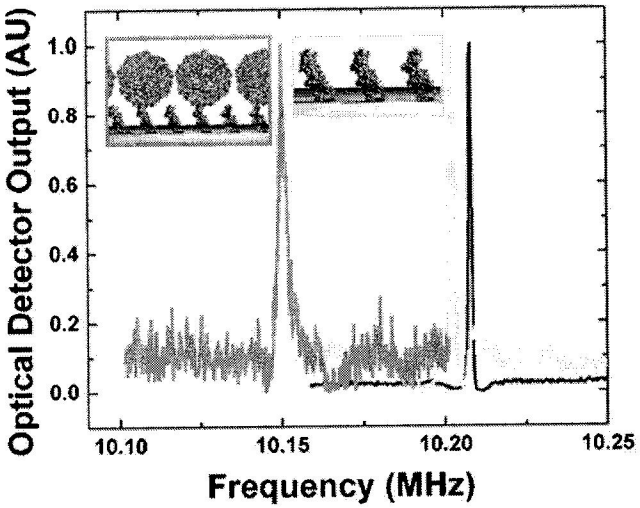

Fig. 5 Example of resonance peaks measured between important reaction steps in the detection of baculovirus particles using nanomechanical cantilevers. The two peaks on the right are taken before (rightmost) and after deposition of the baculovirus-specific antibody layer. The left peak is measured after virus binding; the peak-to-peak shifts are related to the amount of mass added to the cantilever during each step. Reprinted with permission from ref. 69. Copyright 2004, American Institute of Physics.

the moment of inertia for a rectangular beam of width w and thickness t, $I \propto wt^3$, and $A = wt$, one finds that the frequency increases linearly with thickness but has no dependence upon cantilever width.

For resonant sensors, the quality factor is another important quantity that determines absolute mass sensitivity and frequency shift resolution. The quality factor, Q, is defined as $Q = f_0\ \Delta f_{\text{fwhm}}{}^{-1}$, where f_0 is the resonant frequency and Δf_{fwhm} is the full-width at half maximum of the resonance peak. The decreasing width at half-maximum facilitates interpretation of frequency shifts since sharper peaks allow higher resolution of peak frequency shifts. Q is also an important quantity in determining the minimum detectable mass shift of a resonator; this depends on the smallest frequency shift that can be measured. Assuming that a particular fraction of the resonant peak full width at half-maximum can be resolved, Δf in eqn (3) is proportional to $f_0\ Q^{-1}$. Solving for the minimum detectable mass using the above approximation yields the following:

$$\Delta m_{\text{min}} \propto \frac{m}{Q} \tag{5}$$

Decreasing the initial sensor mass, m, and increasing quality factor both reduce the minimum detectable mass of the device. Naturally, the progression to more sensitive resonant sensors has encouraged the development and use of resonant nanoelectromechanical systems. This is in direct contrast to deflection-based microcantilever devices, whose radius of curvature signal requires increasing device length in order to maximize sensitivity. Eqn (5) reveals that the absolute mass sensitivity of resonant MEMS and NEMS sensors operated in a vacuum is primarily a result of the high quality factors compared to air or liquid, where viscous damping losses significantly reduce Q.

Quartz crystal microbalances are large scale resonant sensors, similarly measuring mass by monitoring the resonant frequency of the crystal. Despite having relatively large masses, the sensitivity of QCMs is maintained due to high quality factors. While in vacuum MEMS and NEMS sensors surpass the sensitivity of QCMs, in air or liquid, the QCM typically performs much better. Recently, however, nanomechanical beams are becoming competitive with QCMs in terms of mass sensitivity per unit area.[71] Beams measuring 2 μm × 165 nm × 125 nm were found to resonate at 140 MHz with a quality factor of ~400. Using a conservative estimate that one can resolve frequency shifts that are 10% of the peak width at half maximum, eqn (5) reveals that these devices have a mass per unit area sensitivity of 2.5 ng cm^{-2}.

Alternative pathways to changing resonant frequency

While surface stress constitutes the basis of deflection-based sensors, it is not always an issue for resonance-based sensors and can often go unnoticed. Although several different models have been proposed to describe how surface stress changes the resonant properties of MEMS and NEMS sensors, it remains clear that it is a complex relationship. Surface stresses can affect the stiffness of the resonators and are sometimes considered as a perturbation of the spring constant. An increase in the spring constant, according to eqn (2), would lead to an increase in resonant frequency. If a first order approximation is made similar to that for mass above, a small increase in spring constant, Δk, yields

$$\Delta f = \frac{1}{2} f_0 \left(\frac{\Delta k}{k} - \frac{\Delta m}{m} \right) \tag{6}$$

So, if the percent change in spring constant exceeds that of the mass, Δk then dictates the frequency shift, but can either increase or decrease the resonant frequency. This may become problematic if this change is on the same order of magnitude as the change in m.

Thundat *et al.* fabricated mercury vapor sensors based on resonating silicon nitride cantilevers, coated on one side with gold, to which mercury selectively adsorbs.[22] For sensors with only partial gold coatings, a decrease in resonant frequency was observed with increased exposure, signifying mercury adsorption on the sensor and detection of additional mass. However, in cases where a complete film of gold was used, the frequency was found to increase with exposure, suggesting that mercury adsorption induces a surface stress. A key result is that isolated gold islands increasing in mass produce negligible surface stress, while an entire gold-mercury layer is able to additively overwhelm mass-loading effects and increase the resonance frequency. Functionalizing devices with localized and separated binding sites could possibly remove surface stress effects from resonant mass sensors.

Other models for the effect of surface stress on cantilever resonance have been proposed but the topic is still under much discussion and study. Chen *et al.* modeled the cantilever as a string in order to describe surface stress effects, and they claim that simultaneously measuring deflection and resonance would allow decoupling of the stress and mass effects on resonant frequency.[72] Lu *et al.* question this model, suggesting that it

considerably overestimates external forces and that a taut string is not the best model for a cantilever.[73] They continue to model the cantilever by adding surface stress effects directly into the equations of motion, rather than as a perturbation in spring constant, and find that stress-related frequency shifts are inversely proportional to the Young's modulus and thickness of the beam. The model also shows that binding on both sides of the cantilever, while not producing a static deflection since the stresses should roughly balance, can still change the resonant frequency. They suggest that these effects will only be observed in cases where very thin cantilevers with high quality factors are used and the material system is right for creating large surface stresses. In one example of such a system, exposure of thin, single crystal silicon cantilevers to acetylene or oxygen environments have shown large increases in resonant frequency upon adsorption of the gases.[74]

Recently, a deflection-based sensor for bacterial spores was also resonantly excited in order to measure a frequency shift upon spore attachment.[59] While showing a tip deflection due to surface stress, a negative frequency shift was observed that corresponded to an approximate spore mass which was comparable to previously reported values. This suggests that surface stress either has no effect on the resonance or that it is insignificant compared to mass-related effects.

An additional way in which adsorbing analytes can shift the frequency of a resonant sensor is through the flexural rigidity of the device, EI, where E is Young's modulus and I is the moment of inertia. Recent theoretical work has shown that, depending on the stiffness and thickness of the adsorbate layer compared to that the resonant device, it is plausible that particular material combinations can produce significant positive frequency shifts.[75] Also demonstrated is that flexible materials like SU-8 are more susceptible to these effects and can produce frequency shifts that are several times greater in magnitude than those from mass-loading. Flexural rigidity effects, unlike changes in mass, are also predicted to be greatest when the adsorbate is localized near the clamped end of a cantilever. In a related experimental work, these effects are observed in bacteria adsorption to a resonant cantilever sensor.[76] Using inkjet-deposited droplets of bacteria placed along cantilevers, it was demonstrated that near the clamped end the frequency increases due to stiffness effects, while near the cantilever tip the frequency decreases due to the mass effects. A recent study using cantilevers measuring only 30 nm in thickness demonstrated similar effects.[77] As protein multilayers were deposited on the devices, resonant frequency initially decreased but eventually became a large positive shift as the thickness of the added layers surpassed that of the device. Despite a decrease in the composite Young's modulus of the beam, a two- or threefold increase in device thickness after functionalization can increase the flexural rigidity by a factor of 10 or more, as it is proportional to Et^3. These works suggest that the mechanical properties of the analyte can be important at high coverages.

Resonance actuation and detection mechanisms

There are a wide variety of techniques used to actuate and detect resonance in MEMS and NEMS devices. They can be interchanged and paired based on the specific applications or availability of apparatus. Below we discuss the most common methods of actuation and detection and highlight relative advantages and disadvantages.

Thermal excitation is a simple way in which resonance can be excited. Heat is imparted to the device which then excites resonance by thermal expansion stresses or by using a bilayer of materials with different thermal expansion coefficients. In some cases, even background noise in ambient conditions can excite device oscillation and support sensor operation.[78] Another method, compatible with semiconductor processing techniques, is to fabricate resistors near the resonators that will excite the devices *via* Joule heating. Modulation of the heating source at the resonant frequency of the devices excites oscillation. This has been used to actuate dome-shaped MEMS resonators[79,80] as well as conventional cantilever sensors.[24]

Resonant sensors can also be driven electrostatically or magnetically, and resonance can be monitored using capacitance, encouraging integration with CMOS technology. Out-of-plane resonance has been excited using electrostatic fields between gold films on and near the cantilever.[81] If the cantilever is at a slightly different height than the driving electrode, asymmetry in the electric field lines will create an out-of-plane force, exciting the fundamental cantilever mode. In addition to the fundamental mode, torsional mode actuation has also been demonstrated.[82] Electrostatic excitation has also been achieved for in-plane resonance of cantilevers, using an adjacent driving electrode.[83] In this particular device, resonance was observed using a comb shaped capacitor, and signal amplification was performed on chip using an integrated CMOS circuit.

Magnetically excited devices generally use a microfabricated wire loop on the cantilever on which an alternating current is driven in a static magnetic field to generate out-of-plane excitation using the Lorentz force.[84] Encapsulated cantilevers using this type of electromagnetic excitation have been operated as viscosity sensors in liquid.[85] Doubling back the wire loop near the center of the cantilever creates an opposite Lorentz force from the end and allows excitation of the second flexural mode using the same external magnetic field.[86] Cantilevers made from magnetostrictive materials can also be excited using a varying magnetic field.[87]

Oftentimes, the electromagnetic nature of these excitation mechanisms and their fabrication fit well with piezoresistive detection *via* built-in resistors[24,88] or CMOS circuits.[84] This method is implemented using a Wheatstone bridge, consisting of four resistors, three constant and one variable.[89] The piezoresistive element operates as the variable resistor which changes as the cantilever is strained during deflection or resonance. This technique is sometimes favored compared to others since the resonance probe is built-in, is easily coupled with resistive heating or other on-device excitation methods, and can be encapsulated to protect from a liquid environment.

Another method for excitation of resonance takes advantage of piezoelectric materials. Simply attaching the resonator device chip externally to a driven piezoelectric device can induce resonance. Recently, piezoelectric layers have also been incorporated into multilayer cantilever sensors which can be

used to electrically excite motion, detect resonances, or both.[35,90–92]

In contrast to the above methods that require extra layers of fabrication and addressable electronics, optical excitation and readout offers an external method that can greatly simplify fabrication, minimizing the number of processing steps required. It is also particularly useful for reading large arrays of sensors that would present a formidable problem for other techniques, especially if each device requires electrical connections. A focused laser beam, modulated at device resonance, acts as a localized heat source which thermally excites oscillation.[93,94] Direct illumination of the device is not required, as resonance has been observed in silicon nitride cantilevers when the laser was focused over 160 μm from the clamped end.[94] Another advantage to optical excitation is that it can be applied to a wide variety of device geometries, opening up resonant sensors to creativity and innovation unhindered by electrical integration requirements. For example, parametric amplification of isolated, disk-shaped resonators has been demonstrated using a modulated laser beam, greatly amplifying the signal amplitude and improving force sensitivity.[95]

Optical techniques can also be used to measure device resonance. For larger cantilevers, optical deflection is an option, but as devices become smaller the reflected signal diminishes. However, optimized placement of the detection beam can assist in measuring not only the fundamental mode but also higher modes of cantilever resonance.[96] A more flexible method uses the thin film stack of device layer, sensing medium, and substrate as a Fabry–Pérot interferometer.[19] Using a laser to illuminate a region of the device oscillating out-of-plane, the reflected light will be modulated due to the changing gap height between the sensor and substrate. HeNe laser illumination has been used to detect oscillation in nanomechanical systems with feature sizes significantly less than the wavelength of light (633 nm).[21]

Some recent studies have demonstrated unique methods to detect sensor resonance. One method places an electrode just within the range of motion of a cantilever resonating in-plane so that the cantilever will physically hit the electrode once every cycle.[97] Each contact sends an electrical signal from which resonant frequency can be determined; this technique works hand-in-hand with the electrostatic conditions necessary to excite resonance. A new type of optical detection has been demonstrated using linear silicon nitride optical waveguides that have been patterned into cantilevers.[98] When at rest, light passes through the cantilever and across the relatively small gap between its tip and the remaining waveguide. Device resonance modulates the light that is able to pass through the rest of the waveguide, which can be used to monitor the resonant frequency.

Gas and chemical sensors

Micromechanical devices have been applied as atmospheric gas sensors for several common gases. The detection of water vapor was demonstrated by cantilever frequency shifts due to both mass loading and surface stresses, where phosphoric acid-coated cantilevers decreased in frequency upon H_2O mass loading but one-sided functionalization with gelatin caused an increase in resonant frequency, attributed to surface stress effects.[23] Wang *et al.* reported that oxidation of nanomechanical cantilevers resulted in a significant increase in resonant frequency due to the induced surface stresses on the single crystal silicon devices.[74] Nanomechanical beams coated with palladium have been applied as hydrogen gas sensors for pressures above 10^{-5} Torr, due to the significant uptake of hydrogen in this metal.[99] A micromechanical, membrane-type resonant sensor has been developed for specific detection of carbon dioxide, using a coating of single walled carbon nanotubes as the active layer.[100] The carbon dioxide molecules adsorb to the nanotubes, producing a compressive stress across the device which relieves built in tensile stress, resulting in a decrease in resonant frequency with increased gas concentration.

A unique gas sensor has been developed recently which takes the normally hindering effect of viscous damping and uses it as the sensing mechanism.[101] Knowing the molar mass of the gas being sensed, its pressure can be determined based on the resonant frequency shift of the device. Although complex gas composition analysis was not achieved, detection of carbon dioxide mixed with air was attained for 0–100% concentrations of carbon dioxide. Another particularly clever sensor used deposited films of PtO_2 for detection of hydrogen in air.[102] Hydrogen will chemically react with the platinum oxide, reducing it into platinum, water, and heat, which decreases the amount of mass on the cantilever, producing an increase in resonant frequency.

In addition to atmospheric gas sensing, chemical vapors have also been detected with reasonable success using resonant MEMS and NEMS devices. Mercury vapor, which adsorbs well to gold, has been detected using cantilevers decorated with gold islands; the resonant frequency decreases due to mass-loading upon mercury vapor exposures in the order of a minute.[22] Octane and toluene vapors at concentrations in the order of hundreds of parts per millions have been detected using piezoresistive cantilevers functionalized with a layer of polyetherurethane.[24] More recent work using polyetherurethane and polydimethylsiloxane layers on cantilevers, driven both electrostatically and magnetically, has demonstrated detection of 1-butanol, toluene, and *n*-octane as well as relative detection of binary mixtures of butanol and octane.[103] These devices have also demonstrated the ability to detect other volatile organic vapors, including several alkanes and alcohols.

Resonant biosensors

In the last several years, resonating MEMS and NEMS devices have been increasingly studied as ultrasensitive biological detectors. Ilic *et al.* fabricated cantilevers for the detection of *E. coli* bacteria; as few as 16 cells, or about 6 pg total, were detected in air using ambient thermal noise to excite resonances, despite the low quality factor due to viscous damping.[78] Using cantilevers coated with antibodies specific to the bacteria, resonator frequency shifts were found to increase in magnitude linearly with the number of cells, determined from scanning electron micrographs. In further work with *E. coli*, cantilevers with lengths on the order of 10 micrometres, rather than hundreds of micrometres in the previous study,

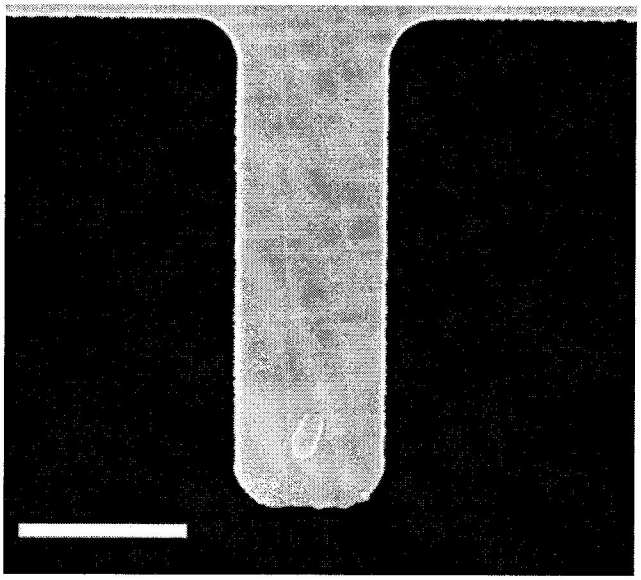

Fig. 6 SEM image taken of a cantilever with a single E. coli bound near the cantilever tip. Actuated in air, this cantilever measured the mass of a single cell to be 665 fg. Scale bar corresponds to 5 μm. Reprinted with permission from ref. 104. Copyright 2001, American Institute of Physics.

were able to measure the frequency shift due to a single cell (665 fg) adsorbed at the end of the cantilever, shown in Fig. 6.[104] The increased sensitivity using the same experimental conditions can be attributed to the reduced oscillator mass. Gold-coated silicon cantilevers, actuated in air, were shown to detect 5.5 fg of a thiol-based SAM.[93]

A creative method using gold nanoparticles was developed in order to amplify very low DNA binding signals from resonating cantilevers.[105] A three-part ssDNA complex bound with thiol–gold chemistry was used, consisting of a bound receptor molecule, the analyte, and a gold-bead functionalized molecule. Following hybridization, silver is selectively nucleated on the gold beads, significantly increasing the bound mass, and thus the resonant signal from the sensor. Although this method requires complicated chemistry, DNA concentrations of 0.05 nM could be detected. Another innovative design placed microfluidic channels inside of a cantilever, which then adds mass by adsorption of analyte internally.[106] Although this device was subject to significant frequency shifts over several minutes, ~1 Hz frequency shifts due to binding of 1 mg mL^{-1} BSA were detectable. Changes in fluid density were also measured using this resonant frequency shift since the microfluidic channel volume was known to be 27 pL.

Pairing resonant detection with SEM, AFM or other imaging techniques allows one to associate frequency shifts, and therefore mass shifts, with the number of large analytes present on the sensors. Surface micromachined devices force a factor of two correction since the cantilever underside can not be observed. Vaccinia viruses were characterized this way using silicon microcantilevers, allowing measurement of average virus mass.[107] The dry mass of *Listeria innocua* bacteria have also been measured with this counting technique, using critical-point drying to dry cantilevers and bacterial cells before resonant detection.[18]

Piezoelectric actuation and detection has been implemented in resonant MEMS biosensors, allowing actuation and detection to take place internally. Unfortunately, these devices require much more fabrication than other sensors for similar sensitivities, due to encapsulation requirements for the electrically active parts. Yeast cells have been detected using piezoelectric layers bonded to stainless steel cantilevers functionalized to adsorb the negatively-charged cells from water.[91] However, the millimetre scale of these devices reduced sensitivity, which was only demonstrated for 1 mg mL^{-1} concentrations of yeast.

Microcantilevers with an encapsulated piezoelectric layer have been used to detect various concentrations of prostate specific antigen, and sensitivity to concentrations as low as 10 pg mL^{-1} were reported.[90] When comparing theoretical mass shifts for these relatively large cantilevers to those found experimentally, experimental values were two orders of magnitude larger than expected. Since bending of the cantilever was observed, they attributed the larger shift to surface stress effects. However, these conclusions contradict the model of Lu *et al.*, which suggests that actuation in air in addition to the thick, multilayer structure of the cantilever significantly reduce the quality factor of the device and its sensitivity to surface stresses.[73]

While single cell detection has been demonstrated with cantilevers operated in air, sensitivities are limited by losses associated with viscous damping. Operation in vacuum removes these losses, leaving only intrinsic loss mechanisms and leading to order of magnitude improvements in quality factor and sensitivity. Indeed, detection of single baculovirus particles, with masses of 1.5 fg, was made possible using polysilicon nanomechanical cantilevers operated in vacuum.[69] Shortly after, a few attograms of thiol-based self-assembled monolayer were detected in vacuum using 4 μm long, 500 nm wide, and 150 nm thick cantilevers.[12] To enhance sensitivity, small gold dots were fabricated at the free end of the nanoscale cantilevers where the mass-related response is greatest, since

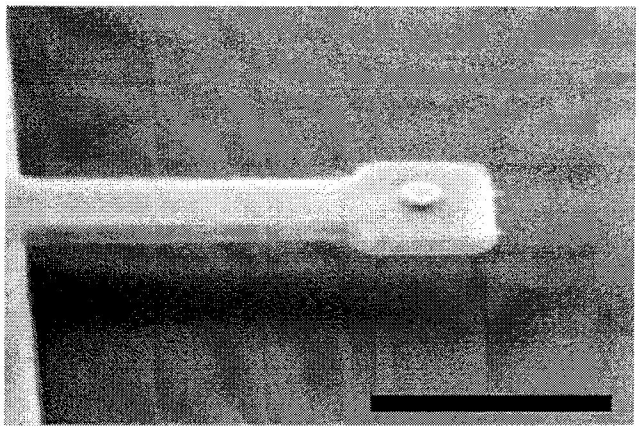

Fig. 7 Image of a specialized cantilever fabricated to specifically bind analytes near the tip of the cantilever in order to maximize the effect of added mass. The nanoscale gold dot can be used with thiol-based binding chemistries to localize analyte binding. This type of device was used to detect attogram quantities of thiol-terminated self-assembled monolayers. Scale bar represents 2 μm. Reprinted with permission from ref. 12. Copyright 2004, American Institute of Physics.

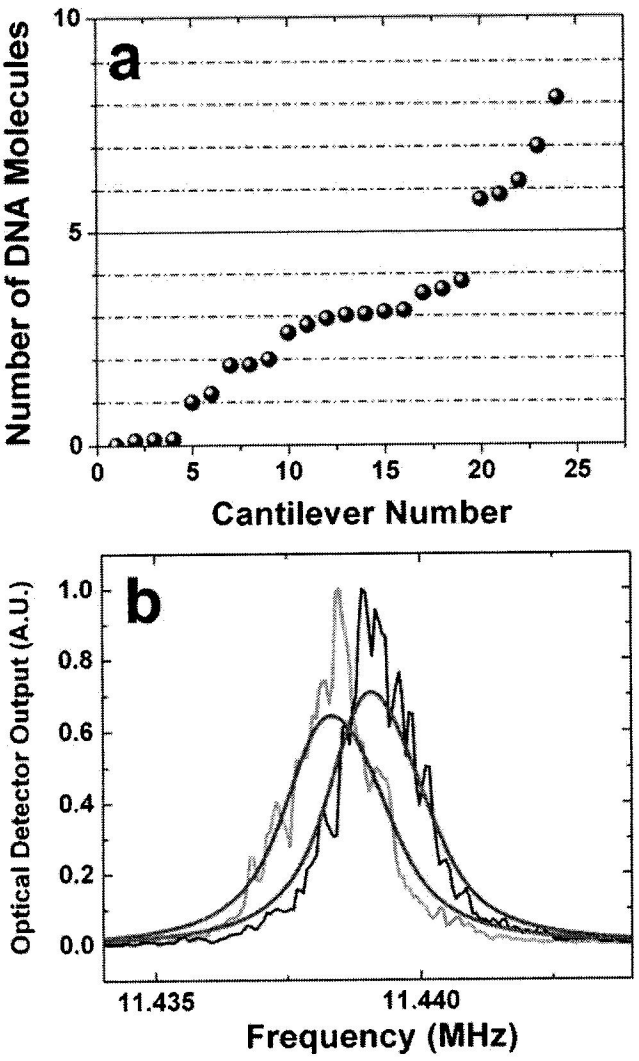

Fig. 8 (a) Cantilever frequency shifts normalized to show the number of single dsDNA molecules bound to each device, demonstrating the ability to count discrete numbers of molecules. (b) Resonant peaks and fitted curves taken before and after DNA binding show the frequency shift resulting from single molecule binding. Reprinted with permission from ref 13. Copyright 2005, American Chemical Society.

the effective mass added to the cantilever decreases as the mass moves closer to the clamped end of the cantilever. Fig. 7 shows an SEM micrograph of such a cantilever patterned with a single gold dot. Recently, nanomechanical resonant biosensors have pushed the limits of sensitivity to the point of single molecule detection. Using cantilevers functionalized similarly with a gold dot, single dsDNA molecules (1587 bp) with a mass of 1.65 ag were detected.[13] Observing many cantilevers revealed approximately discrete frequency jumps corresponding to a handful of DNA molecules. Normalizing these shifts to the frequency shift from a single binding event enables counting of DNA molecules bound to a particular cantilever, shown in Fig. 8(a); the frequency peaks before and after single molecule binding are given in Fig. 8(b). A summary of recent achievements in resonating biological sensors is given in Table 2.

Opportunities for improved sensors

There is room for optimizing resonant MEMS and NEMS sensors and improving their operation outside of vacuum where they become susceptible to viscous damping. Biological sensors would benefit greatly from such improvements, allowing operation in more biologically appropriate environments and real-time observation of resonant frequency shifts. Signal amplification is of key interest, especially for ultrasensitive detection. Besides using additional mass labels,[105] integrated CMOS electronics can amplify electronic resonance signals on chip. In-plane resonance of nanomechanical cantilevers in air has demonstrated an excellent mass sensitivity when paired with integrated CMOS circuitry, measuring a 57 fg mass.[83] More generally, enhanced signals are obtained from devices with higher quality factors, which give sharper resonance peaks and thus improved resolution. In addition, the existence of many resonance modes for a given device lends increased versatility and room for creativity to resonant sensors when compared to deflection-based sensors.

Continually reducing device dimensions in order to decrease resonator mass has generally been a fruitful approach to improving the absolute mass sensitivity of these sensors, as shown in eqn (5). An underlying assumption applied to most resonant sensor schemes is that the adsorbed film is much thinner than the cantilever thickness, which makes changes in

Table 2 Examples of Resonance-based Biological Sensor Achievements

Analyte	Minimum detected	Device layer	Actuation/detection	Medium	Ref.
dsDNA	1.65 ag (single dsDNA)	Silicon nitride	Optical/optical interference	Vacuum	13
Thiol SAMs	6.3 ag	Silicon nitride	Piezoelectric/optical interference	Vacuum	12
Baculovirus	1.5 fg (single virus)	Polycrystalline silicon	Piezoelectric/optical interference	Vacuum	69
Thiol SAMs	5.5 fg	silicon	Optical/optical interference	Air	93
Glycerin	57 fg	Polycrystalline silicon	Electrostatic/capacitive	Air	83
E. Coli	0.67 pg (single cell)	Silicon nitride	Ambient/optical reflection	Air	104
E. Coli	6 pg (16 cells)	Silicon nitride	Ambient/optical reflection	Air	78
Biotinylated latex beads	7 ng	Silicon	Piezoelectric/optical reflection	Liquid	130
PSA	10 pg mL^{-1}	Lead zirconate titanate/silicon nitride	Piezoelectric	Air	90
Myoglobin	~1 ng mL^{-1}	Lead zirconate titanate/silicon	Piezoelectric	Air	35
PSA	1 ng mL^{-1}	Lead zirconate titanate/silicon nitride	Piezoelectric/optical reflection	Liquid	92
BSA	1 mg mL^{-1}	Silicon nitride	Electrostatic/optical reflection	Air	106
Yeast cell	1 mg mL^{-1}	Lead zirconate titanate/steel	Piezoelectric	Air/water	91
ssDNA	0.05 nM	Silicon nitride	AFM tapping mode	Air	105
Goat anti-mouse IgG	0.7 nM	Silicon	Electrostatic/optical reflection	Vacuum	128

mechanical properties of the beam negligible. However, once the device thickness approaches the order of functional layer thickness, the system can behave more like a composite structure rather than a simple microbalance. In this regime, the frequency behavior of resonant devices is sensitive to more than just added mass. Recently, resonators fabricated from single atomic layers of graphene were demonstrated, representing a limit of minimizing sensor mass.[108]

Viscous damping is by far the greatest loss mechanism responsible for reduction of quality factors by a few orders of magnitude in air, while the effect in liquid is generally greater. Operation in vacuum eliminates viscous damping, revealing other mechanisms such as surface and clamping (support) loss. Surface losses are particularly important for NEMS devices as they exhibit large surface to volume ratios in smaller and more sensitive structures. Particular surface chemistries used for these devices can also have a significant effect on quality factor that is unrelated to mass loading or surface stress; recent work has suggested that these losses are from surface defects which can be eliminated by altering the surface termination.[109] In further work, passivating resonator surfaces with methyl groups was shown to be more stable over time than other alkyl terminations or hydrogen passivated surfaces.[110] Ekinci *et al.* have tested the limits of mass sensing based on fundamental noise processes. However, these findings are only applicable at cryogenic temperatures in ultra-high vacuum, as viscous damping of air or water found in many biological sensor systems render these losses negligible.[111] However, minimizing these losses at such low temperature and pressure has allowed the nanomechanical detection of only 7 zeptograms (10^{-21} g) of adsorbed xenon, or roughly 30 Xe atoms.[15]

Although loss mechanisms are not entirely understood, much work has focused on the effect of the many device parameters that affect Q. Yasumura *et al.* studied the quality factors of single and poly-crystalline silicon and silicon nitride cantilevers and found that it increased with device thickness, while no consistent trends with cantilever length were observed.[112] An interesting dependence of Q on temperature was found, with the highest values at cryogenic temperatures and a minimum near 130 K. Although low temperatures are not realistic for commercialized biosensors, the quality factor does increase to another maximum near room temperature. Another issue with these devices is that additional layers introduce increased loss pathways and reduce quality factor. Gold layers, common in thiol-based chemistries and single-sided binding for deflection based sensors, can reduce cantilever quality factors by an order of magnitude for films only 100 nm thick.[113,114]

Fabrication processes can also significantly affect quality factors of resonant sensors. Although low stress silicon nitride is most commonly used for MEMS devices, changing the silicon to nitrogen stoichiometry can introduce high stress into the device layer, which may result in devices with very high quality factors. Quality factors greater than 200 000 were recently demonstrated using doubly-clamped, nanomechanical oscillators made from high stress silicon nitride.[21] This is a remarkable result when taking into account the large surface to volume ratio of these nanostrings, with both widths and thicknesses on the order of 100 nm. It has also been shown that single crystal silicon devices have increased quality factors when flash heated.[74] Thermally annealing resonators with a low power ($\sim$mW) laser, a chip-friendly and localized method compared to wafer level heating, has also been used to improve quality factors by an order of magnitude.[115] In addition, recent work has shown that simply changing a chemical etchant can affect the fracture strength of silicon nanobeams, providing further evidence for how much influence fabrication can have on MEMS and NEMS operation.[116]

Recently, more attention has been given to the higher modes of resonating cantilevers, and significant advantages over the fundamental mode have been found. Dohn *et al.* point out that higher harmonics of the out-of-plane mode introduce nodes in the resonance, which decrease the effective mass of the cantilever and improve its sensitivity.[117] They also measured the frequency response of a cantilever to a 60 pg gold bead, which is accurately positioned along the resonator using a piezoelectric micromanipulator. In exploring the positional sensitivity of these out-of-plane harmonic modes, higher modes were found to be increasingly sensitive to mass placed all along the cantilever compared to the first mode, where sensitivity is considerably limited as the mass moves closer to the clamped end. This effect has also been experimentally observed in the detection of mercury vapor using higher order modes of resonance.[118] While cantilevers functionalized only at the tip show increasing frequency shifts with higher modes, the responses for entirely functionalized devices show more pronounced improvements using the higher modes, changing frequency more rapidly and saturating at larger values of frequency shift.

Higher resonant modes have also demonstrated larger quality factors in several different experiments using resonators actuated in air.[113,117–120] In addition to the higher harmonics of the out-of-plane mode, the lateral, in-plane mode as well as the torsional mode have also exhibited larger frequency shifts and quality factors than the fundamental bending mode.[119] These improvements would lead to increased mass sensitivities for detection in air, suggesting that higher modes are less susceptible to viscous damping losses.

The double paddle oscillator,[120,121] a millimetre scale cantilever decorated with two large, wing-like paddles on each side and a smaller head at the end, is an example of another device showing improved response using a higher mode of resonance. The second, asymmetrical torsion mode, where the wings are twisting out of phase, demonstrated a reduction of internal friction, Q^{-1}, by several orders of magnitude, corresponding to quality factors approaching 10^8 at temperatures below 40 K.[120] This can be partially attributed to a reduction in support loss, which is minimized as the center-of-mass motion of the resonator is reduced and the torsional forces at the support are reduced, accomplished by the asymmetrically balanced twisting.[68] These devices have been particularly useful in studying the properties of amorphous thin films.[122,123] Although these large devices may not be applicable as biosensors due to their comparably large masses, nanoscale analogues may prove useful for improved quality factor and mass sensitivity.

Another unique advantage of resonance-based MEMS and NEMS biosensors over deflection based systems is that devices can be of arbitrary shape, allowing more flexible applications

utilizing higher or unique resonant modes, like that of the double-paddle oscillator. Recently, two microcantilevers were fabricated from a gold foil, and resonant coupling of the devices was built into the design using a slightly larger overhang between the two cantilevers.[124] The symmetric (in phase) and asymmetric (out of phase) fundamental modes for this device have resonant frequencies separated by about 0.5 kHz and can be identified by observing the phase as a function of frequency. What makes these devices unique is if added mass is unequally distributed to the cantilevers, the two resonance peaks will significantly change in character, allowing inherent background subtraction and improved sensitivity. Another creative resonant sensor has been fabricated with a novel method of detecting resonance, by hard contact.[97] The SiO_2 device is coated in platinum and capacitively driven in the in-plane resonance mode. When resonating, the cantilever makes an electrical contact to the sensing electrode which sends digital-like current pulse signals, allowing the number of cycles to be directly counted in order to measure the resonant frequency. Frequency shifts due to 0.5 pg of additional mass were easily resolvable while actuating these devices in ambient conditions.

Potential for microfluidic operation

The increasing research and development of lab-on-a-chip devices for complete analysis of small chemical and biological sample volumes is driving the miniaturization of many analytical tools. Due to their small sizes, MEMS and NEMS biosensors are good candidates for integration into microfluidic lab-on-a-chip systems. Resonant devices are particularly promising as the more sensitive devices are less than 10 micrometres in length and on the order of 100 nm thick. Aubin *et al.* have fabricated silicon nitride NEMS resonator arrays inside 150 μm wide microfluidic channels.[17] Encapsulation using a borosilicate glass wafer allowed optical excitation and readout of device resonance. Flowing several liquids through the microchannels and drying with nitrogen did not induce device stiction or degrade resonator function. Viscous damping was avoided by pumping the channels down to pressures near a milliTorr, where device quality factors were approximately 2000. One can envision many parallel microfluidic channels with several resonators in each, allowing multiplexed resonant mass detection of many different analytes from the same sample.

For ideal operation of resonant devices in microfluidics, viscous damping must be overcome, as it is by far what limits the quality factor most. A reduction in quality factor of two to three orders of magnitude operating in liquid rather than vacuum is not uncommon. Intuitively, viscous damping increases with pressure in air or with viscosity in liquid. One way in which viscosity affects resonance is by forming a thin film of fluid around the device, with a thickness that is proportional to the square root of the viscosity divided by the operating frequency. Since this layer moves with the cantilever, it is effectively increasing device mass and thus reducing sensitivity. However, the thickness of this film can be reduced by using higher frequency devices, or higher modes of the same device. Also, if a biological entity is to be detected from a complex fluid like serum, the background particulates can also effect device operation, especially in optical systems.[125] Primarily, mesoscale particles such as platelets, bacteria, or other organisms will scatter light used to actuate or probe the devices, while momentum transfer between particles and devices can also be a source of noise. This work suggests that complex samples should be pre-concentrated or refined prior to introduction to the biosensors, a feature that can be integrated in microfluidics.

Recently, Basak *et al.* have shed light on the process of viscous damping of resonating cantilevers using finite element analysis.[126] In studying a few different cantilever shapes, their model suggests that wider devices have higher quality factors, and that slotted or necked cantilevers result in reduced quality factors. Observing the fluid shear as a result of these device geometries revealed that shear is very high at all of the edges of the device, which are more numerous in slotted or necked cantilevers, resulting in higher energy dissipation and lower values for Q. Squeeze film effects were also investigated, which become important when the gap between suspended cantilevers and the substrate become comparable to the thickness of the water boundary layer surrounding the cantilever. The torsional mode, operating at a higher frequency than the first bending mode, not only experiences less bending towards the substrate, but has a thinner bound water layer, and can thus approach closer to the surface. In addition, the quality factor was found to increase with mode number, analogous to the improved performance of higher modes for resonators operated in air.[113,117–120] These results have significant implications on the use of surface micromachined resonators in fluid.

Rather than operating resonators in microfluidics and dealing with viscous damping, Burg and Manalis have turned the problem inside-out, operating microfluidics in resonators.[106] This system is advantageous because device actuation in vacuum is still viable, allowing for high quality factors and negligible viscous damping. In these devices, the mass change due to binding of material of different density than the solution is detected. More recently, T. P. Burg *et al.* have fabricated these cantilevered microfluidic channels as part of a vacuum-packaged system.[127] The microfluidic resonators were able to discern changes in fluid density with a sensitivity of a 4% decrease in frequency per unit density (g cm^{-3}), which corresponds to a sensitivity to surface bound mass of 0.8 ppm (g cm^{-2})$^{-1}$. Exposure to 1 mg mL^{-1} avidin solution resulted in a ~2 Hz (60 ppm) frequency shift, corresponding to a total detected mass of 75 pg. For fluid-filled devices packaged at pressures near a Torr, their quality factors were on the order of 500, a great improvement over MEMS and NEMS resonators operated in liquid; devices operated in a vacuum chamber exhibited quality factors of over 10 000.

Cantilevered microfluidic devices encapsulated in vacuum have also shown the ability to measure both masses flowing through the cantilever as well as masses adsorbing to functionalized channel walls in the resonator.[128] Large and massive objects, such as bacteria or nanoparticles, have been measured while flowing through the channels, causing a frequency shift depending on distance from the cantilever support. The short time scales of the reversible frequency shifts

permit counting of masses and further statistical analysis. They point out that these resonators, interfaced with fluid samples, are able to detect mass changes per unit area of ~ 10 pg cm^{-2}, which is roughly 100 times more sensitive than QCMs.

Whether resonators are operated in microfluidic chips or the microfluidic channels themselves are used as resonators, integration of these sensors within microfluidic systems devices could be advantageous. MEMS and NEMS sensors could benefit from the wealth of microfluidic and lab-on-a-chip device technologies. On-chip separation techniques would be useful in allowing biologically relevant and easily acquirable samples such as blood or urine to be directly loaded into the fluidic system. In addition, pre-concentration techniques could be particularly useful in the detection of very dilute analytes.

Despite viscous damping limitations, a few resonant sensors have been operated in liquid with some success. Relatively large cantilevers, 200 μm long and 7.7 μm thick, of varying widths have been operated in a fluidic cell with quality factors from 10 to 20.[85] Increasing the cantilever width from 50 to about 200 μm improved the quality factors by about a factor of two. In addition, they demonstrated a Lorentz force actuation mechanism with piezoresistive detection, all encapsulated on the cantilever. Piezoelectric cantilevers have shown some promise for working in fluids; despite their typically low Q in vacuum, operation in fluid does not drastically reduce the already low quality factor. One particular work demonstrates detection of ng mL^{-1} concentrations of prostate specific antigen in fluid.[92]

Operation of radio frequency resonators, on the order of 10 to 100 MHz, has been demonstrated in liquid using optical excitation and detection.[71] Nanostring devices, ~ 120 nm thick with widths as small as 100 nm, absorb sufficient heat from laser actuation to resonate and produce enough signal when used as a Fabry–Perot interferometer. Another group has shown optical excitation in fluid, using a laser focused on regions of high curvature in the resonant mode shape.[129] Recent experiments detecting latex beads using biotin–streptavidin chemistry achieved time-resolved measurement of ~ 7 ng with resonant cantilevers in liquid.[130] Using the 11th, 12th and 13th flexural modes of 500 μm long silicon cantilevers, they take advantage of predicted higher sensitivity due to reduction of the liquid layer bound to the cantilever added liquid mass. The authors monitor the eigenfrequencies of the modes, defined by turning points in the phase *vs.* frequency curve, rather than typical amplitude *vs.* frequency peaks.

Comparison of deflection- and resonance-based sensing techniques

Detection limit

Resonance-based biosensors have exceeded the absolute mass detection capabilities of deflection-based devices, supporting single cell, virus, and double-stranded DNA molecule detection. Analytes on the order of attograms have been weighed with nanomechanical sensors using frequency shift measurements. This detection regime is inaccessible to deflecting biosensors, since a sufficient number of binding events must occur in order to produce a surface stress strong enough to significantly bend the cantilever. One work found that approximately $\sim 2 \times 10^{10}$ binding events per mm^2 were required on a cantilever surface in order to detect deflection.[51] There is also evidence that disperse adsorption may not produce enough surface stress to deflect cantilevers.[22] However, these ultrasensitive resonant devices must be operated in vacuum to avoid viscous fluid damping.

Operation in fluid and interfacing with microfluidics

Deflection-based devices offer an important advantage over resonators in that they work well in fluids, since static bending of the devices is not subject to viscous damping. In turn, this allows real-time measurement of cantilever deflection while performing the experimental chemistry. However, there have been recent advances in resonant sensing that are improving the sensitivity of these devices in fluids. The use of higher resonant modes of sensors operated in air has been demonstrated to improve sensitivity and reduce viscous losses.[113,117–120] Results showing higher quality factors for higher resonant modes suggest similar improvements for devices used in liquids.[126] The higher resonant frequencies associated with higher modes also help to reduce the hydrodynamic loading of the devices, which will further increase sensitivity. Recent work to put fluidic channels inside of cantilevers shows promise for allowing real-time biosensing from solution with the high sensitivity of resonant sensors operated in vacuum.[106,128]

Much would be gained by integrating these sensors into a microfluidic system as a part of an on-chip system with concentrating, filtering, and other components built in. For such lab-on-a-chip applications, deflection-based sensors may be used but would require some additional attention. Because the sensitivity of deflecting cantilevers is proportional to the square of the length they tend to be long. Avoiding stiction creates constraints in microfluidic integration. While resonant sensors are small enough to be placed at a high density within microfluidic channels, viscous damping must still be addressed.

Signal-to-noise considerations

A range of noise processes, ambient fluctuations and chemical processes have a significant effect on sensitivity. Some noise effects result from fluctuations in the mechanical elements, but the detection systems in many cases may be a significant source of noise. For instance, in optical measurement systems, there is noise in the intensity and phase of the detected signal, in addition to photodetector shot noise.[131] Due to the DC nature of their signals, static deflection-based systems are particularly susceptible to $1/f$ noise, also referred to as flicker noise. In fact, this noise is often the main factor which limits device sensitivity by increasing the value of the minimum detectable deflection.[132,133] Though this noise is not entirely understood, some studies have observed that flicker noise in piezoresistive cantilevers is dependent on geometry, dopant concentration and distribution, as well as thermal annealing treatments.[133,134] While temperature control systems can be used, small thermal fluctuations and drift may have a significant effect on metalized cantilevers, where the gold coating used for

single-sided functionalization has a significantly different thermal expansion coefficient relative to the cantilever. Vibrations and thermal variations can also affect resonant devices.

In resonant detection systems, the frequency width of the resonant response is the fundamental instrumental limit, and this feature, usually discussed in terms of the mechanical quality factor, Q, can be influenced by many factors. As discussed above, in fluids the viscous damping is the primary dissipation mechanism that limits the Q and broadens the resonance. This factor motivates the device designs that optimize the ratio of oscillator mass to Q. In the low pressure regime, viscous damping is eliminated but chemical coatings can also contribute to mechanical losses and degrade the quality factor.

In many cases the mechanical device and instrumental limitations are not the most significant limitations in the signal-to-noise ratio. Chemical specificity and associated non-specific binding of non-target compounds is the most significant limit in sensing performance. Dealing with chemical processes compatible with the NEMS or MEMS devices is important.

Conclusions

Micro- and nanoelectromechanical systems have been studied and developed into increasingly sensitive gas, chemical, and biological sensors. The versatility of these sensors is limited only by the existence of surface chemistries or functionalization techniques that selectively bind analytes of interest. In addition, small-scale, label-free biosensors are becoming potential competitors to microarray and protein assay technologies due to their small size, ease of fabrication in large arrays, and high sensitivities.

Future challenges to MEMS and NEMS biosensors include limiting non-specific binding to an extent where analytes may be detected from serum or other complex fluids, as well as circumventing or greatly reducing the effects of viscous damping in the case of resonant sensors. Significant progress has been made towards resonant biosensor operation in fluids, improving mass sensitivities despite being limited by viscous damping. Integration of these devices into microfluidics and on-chip total analysis systems is within reach and holds great promise for sensitive mass detection in fluids. The encouraging results in recent work suggest that complete development of resonant biological sensors should have a significant impact on medicine, proteomics, and many other fields.

Acknowledgements

P.S.W. gratefully acknowledges support from the Department of Defence *via* the National Defence Science and Engineering Graduate Fellowship. We thank K. L. Aubin and S. S. Verbridge for helpful discussions.

References

1 G. Binnig, C. F. Quate and C. Gerber, *Phys. Rev. Lett.*, 1986, **56**(9), 930–933.
2 M. M. Elrick, J. L. Walgren, M. D. Mitchell and D. C. Thompson, *Bas. Clin. Pharmacol. Toxicol.*, 2006, **98**, 432–441.
3 C. Hempen and U. Karst, *Anal. Bioanal. Chem.*, 2006, **384**, 572–583.
4 N. Ramachandran, D. N. Larson, P. R. H. Stark, E. Hainsworth and J. LaBaer, *FEBS J.*, 2005, **272**, 5412–5425.
5 M. A. Cooper, *Anal. Bioanal. Chem.*, 2003, **377**, 834–842.
6 J. Homola, S. S. Yee and G. Gauglitz, *Sens. Actuators, B*, 1999, **54**, 3–15.
7 Q-Sense AB, Västra Frölunda, Sweden. Available online: http://www.q-sense.com.
8 A. W. Warner, in *Ultra Micro Weight Determination in Controlled Environments*, ed. S. P. Wolsky and E. J. Zdanuk, Interscience, New York, 1969, ch. 5, pp. 137–161.
9 H. G. Craighead, *Science*, 2000, **290**, 1532–1535.
10 K. L. Ekinci and M. L. Roukes, *Rev. Sci. Instrum.*, 2005, **76**(6), 061101.
11 W. P. King, T. W. Kenny, K. E. Goodson, G. L. W. Cross, M. Despont, U. T. Dürig, H. Rothuizen, G. Binnig and P. Vettiger, *J. Microelectromech. Syst.*, 2002, **11**(6), 765–774.
12 B. Ilic, H. G. Craighead, S. Krylov, W. Senaratne, C. Ober and P. Neuzil, *J. Appl. Phys.*, 2004, **95**(7), 3694–3703.
13 B. Ilic, Y. Yang, K. Aubin, R. Reichenbach, S. Krylov and H. G. Craighead, *Nano Lett.*, 2005, **5**(5), 925–929.
14 K. L. Ekinci, X. M. H. Huang and M. L. Roukes, *Appl. Phys. Lett.*, 2004, **84**(22), 4469–4471.
15 Y. T. Yang, C. Callegari, X. L. Feng, K. L. Ekinci and M. L. Roukes, *Nano Lett.*, 2006, **6**(4), 583–586.
16 J. Bishop, A. Chagovetz and S. Blair, *Nanotechnology*, 2006, **17**, 2442–2448.
17 K. L. Aubin, S. Park, J. Huang, J. Huang, B. R. Ilic and H. G. Craighead, *Proc. 4th IEEE Conf. Sens.*, 2005, Irvine, CA, USA, 720–722.
18 A. Gupta, D. Akin and R. Bashir, *J. Vac. Sci. Technol., B*, 2004, **22**(6), 2785–2791.
19 D. W. Carr and H. G. Craighead, *J. Vac. Sci. Technol., B*, 1997, **15**(6), 2760–2763.
20 D. A. Czaplewski, S. S. Verbridge, J. Kameoka and H. G. Craighead, *Nano Lett.*, 2004, **4**(3), 437–439.
21 S. S. Verbridge, J. M. Parpia, R. B. Reichenbach, L. M. Bellan and H. G. Craighead, *J. Appl. Phys.*, 2006, **99**(12), 124304.
22 T. Thundat, E. A. Wachter, S. L. Sharp and R. J. Warmack, *Appl. Phys. Lett.*, 1995, **66**(13), 1695–1697.
23 T. Thundat, G. Y. Chen, R. J. Warmack, D. P. Allison and E. A. Wachter, *Anal. Chem.*, 1995, **67**(3), 519–521.
24 D. Lange, C. Hagleitner, A. Hierlemann, O. Brand and H. Baltes, *Anal. Chem.*, 2002, **74**(13), 3084–3095.
25 M. K. Baller, H. P. Lang, J. Fritz, Ch. Gerger, J. K. Gimzewski, U. Dreshler, H. Rothuizen, M. Despont, P. Vettiger, F. M. Battiston, J. P. Ramseyer, P. Fornaro, E. Meyer and H.-J. Güntherodt, *Ultramicroscopy*, 2000, **82**, 1–9.
26 J. Fritz, M. K. Baller, H. P. Lang, H. Rothuizen, P. Vettiger, E. Meyer, H.-J. Güntherodt, Ch. Gerber and J. K. Gimzewski, *Science*, 2000, **288**, 316–318.
27 A. Subramanian, P. I. Oden, S. J. Kennel, K. B. Jacobson, R. J. Warmack, T. Thundat and M. J. Doktycz, *Appl. Phys. Lett.*, 2002, **81**(2), 385–387.
28 S.-J. Hyun, H.-S. Kim, Y.-J. Kim and H.-I. Jung, *Sens. Actuators, B*, 2006, **117**, 415–419.
29 C. A. Savran, S. M. Knudsen, A. D. Ellington and S. R. Manalis, *Anal. Chem.*, 2004, **76**(11), 3194–3198.
30 S. S. Iqbal, M. W. Mayo, J. G. Bruno, B. V. Bronk, C. A. Batt and J. P. Chambers, *Biosens. Bioelectron.*, 2000, **15**, 549–578.
31 H. Xu, X. Zhao, C. Grant, J. R. Liu, D. E. Williams and J. Penfold, *Langmuir*, 2006, **22**(14), 6313–6320.
32 B. Lu, M. R. Smyth and R. O'Kennedy, *Analyst*, 1996, **121**, 29R–32R.
33 M. Friedel, A. Baumketner and J.-E. Shea, *Proc. Natl. Acad. Sci. U. S. A.*, 2006, **103**(22), 8396–8401.
34 R. A. Vijayendran and D. E. Leckband, *Anal. Chem.*, 2001, **73**(3), 471–480.
35 G. Y. Kang, G. Y. Han, J. Y Kang, I.-H. Cho, H.-H. Park, S.-H. Paek and T. S. Kim, *Sens. Actuators, B*, 2006, **117**, 332–338.
36 N. Backmann, C. Zahnd, F. Huber, A. Bietsch, A. Plückthun, H.-P. Lang, H.-J. Güntherodt, M. Hegner and Ch. Gerber, *Proc. Natl. Acad. Sci. U. S. A.*, 2005, **102**(41), 14587–14592.

37 P. Peluso, D. S. Wilson, D. Do, H. Tran, M. Venkatasubbaiah, D. Quincy, B. Heidecker, K. Poindexter, N. Tolani, M. Phelan, K. Witte, L. S. Jung, P. Wagner and S. Nock, *Anal. Biochem.*, 2003, **312**, 113–124.
38 C. Wingren, C. Steinhauer, J. Ingvarsson, E. Persson, K. Larsson and C. A. K. Borrebaeck, *Proteomics*, 2005, **5**, 1281–1291.
39 H.-F. Ji, K. M. Hansen, Z. Hu and T. Thundat, *Sens. Actuators, B*, 2001, **72**, 233–238.
40 N. V. Lavrik, M. J. Sepaniak and P. G. Datskos, *Rev. Sci. Instrum.*, 2004, **75**(7), 2229–2253.
41 C. Ziegler, *Anal. Bioanal. Chem.*, 2004, **379**, 946–959.
42 L. G. Carrascosa, M. Moreno, M. Alvarez and L. M. Lechuga, *TrAC, Trends Anal. Chem.*, 2006, **25**(3), 196–206.
43 G. G. Stoney, *Proc. R. Soc. London, Ser. A*, 1909, **82**(553), 172–175.
44 M. Calleja, J. Tamayo, M. Nordström and A. Boisen, *Appl. Phys. Lett.*, 2006, **88**(11), 113901.
45 L. Gammelgaard, P. A. Rasmussen, M. Calleja, P. Vettiger and A. Boisen, *Appl. Phys. Lett.*, 2006, **88**(11), 113508.
46 J. H. T. Ransley, M. Watari, D. Sukumaran, R. A. McKendry and A. A. Seshia, *Microelectron. Eng.*, 2006, **83**, 1621–1625.
47 Y. Tang, J. Fang, X. Yan and H.-F. Ji, *Sens. Actuators, B*, 2004, **97**, 109–113.
48 R. Berger, E. Delamarche, H. P. Lang, C. Gerber, J. K. Gimzewski, E. Meyer and H.-J. Güntherodt, *Science*, 1997, **276**, 2021–2024.
49 G. Wu, R. H. Datar, K. M. Hansen, T. Thundat, R. J. Cote and A. Majumdar, *Nat. Biotechnol.*, 2001, **19**, 856–860.
50 G. Wu, H. Ji, K. Hansen, T. Thundat, R. Datar, R. Cote, M. F. Hagan, A. K. Chakraborty and A. Majumdar, *Proc. Natl. Acad. Sci. U. S. A.*, 2001, **98**(4), 1560–1564.
51 R. McKendry, J. Zhang, Y. Arntz, T. Strunz, M. Hegner, H. P. Lang, M. K. Baller, U. Certa, E. Meyer, H.-J. Güntherodt and Ch. Gerber, *Proc. Natl. Acad. Sci. U. S. A.*, 2002, **99**(15), 9783–9788.
52 M. F. Hagan, A. Majumdar and A. K. Chakraborty, *J. Phys. Chem. B*, 2002, **106**(39), 10163–10173.
53 J. C. Stachowiak, M. Yue, K. Castelino, A. Chakraborty and A. Majumdar, *Langmuir*, 2006, **22**(1), 263–268.
54 R. Bashir, J. Z. Hilt, O. Elibol, A. Gupta and N. A. Peppas, *Appl. Phys. Lett.*, 2002, **81**(16), 3091–3093.
55 S.-H. Lim, D. Raorane, S. Satyanarayana and A. Majumdar, *Sens. Actuators, B*, 2006, **119**, 466–474.
56 R. A. Potyrailo, A. Leach, W. G. Morris and S. K. Gamage, *Anal. Chem.*, 2006, **78**(16), 5633–5638.
57 P. Li, X. Li, G. Zuo, J. Liu, Y. Wang, M. Liu and D. Jin, *Appl. Phys. Lett.*, 2006, **89**(7), 074104.
58 B. L. Weeks, J. Camarero, A. Noy, A. E. Miller, L. Stanker and J. J. De Yoreo, *Scanning*, 2003, **25**, 297–299.
59 B. Dhayal, W. A. Henne, D. D. Doomeweerd, R. G. Reifenberger and P. S. Low, *J. Am. Chem. Soc.*, 2006, **128**, 3716–3721.
60 Y. Arntz, J. D. Seelig, H. P. Lang, J. Zhang, P. Hunziker, J. P. Ramseyer, E. Meyer, M. Hegner and Ch. Gerber, *Nanotechnology*, 2003, **14**, 86–90.
61 F. Huber, M. Hegner, Ch. Gerber, H.-J. Güntherodt and H. P. Lang, *Biosens. Bioelectron.*, 2006, **21**, 1599–1605.
62 K. W. Wee, H. Y. Kang, J. Park, J. Y. Kang, D. S. Yoon, J. H. Park and T. S. Kim, *Biosens. Bioelectron.*, 2005, **20**, 1932–1938.
63 R. Mukhopadhyay, M. Lorentzen, J. Kjems and F. Besenbacher, *Langmuir*, 2005, **21**(18), 8400–8408.
64 G. Shekhawat, S.-H. Tark and V. P. Dravid, *Science*, 2006, **311**, 1592–1595.
65 W. Shu, D. Liu, M. Watari, C. K. Riener, T. Strunz, M. E. Wellend, S. Balasubramanian and R. A. McKendry, *J. Am. Chem. Soc.*, 2005, **127**(48), 17054–17060.
66 R. Mukhopadhyay, V. V. Sumbayev, M. Lorentzen, J. Kjems, P. A. Andreasen and F. Besenbacher, *Nano Lett.*, 2005, **5**(12), 2385–2388.
67 T. Braun, N. Backmann, M. Vögtli, A. Bietsch, A. Engel, H.-P. Lang, C. Gerber and M. Hegner, *Biophys. J.*, 2006, **90**(8), 2970–2977.
68 G. Stemme, *J. Micromech. Microeng.*, 1991, **1**, 113–125.
69 B. Ilic, Y. Yang and H. G. Craighead, *Appl. Phys. Lett.*, 2004, **85**(13), 2604–2606.
70 W. Weaver Jr., S. P. Timoshenko and D. H. Young, *Vibration Problems in Engineering*, Wiley-Interscience, New York, 5th edn, 1990, ch. 5, pp. 427–428.
71 S. S. Verbridge, L. M. Bellan, J. M. Parpia and H. G. Craighead, *Nano Lett.*, 2006, **6**(9), 2109–2114.
72 G. Y. Chen, T. Thundat, E. A. Wachter and R. J. Warmack, *J. Appl. Phys.*, 1995, **77**(8), 3618–3622.
73 P. Lu, H. P. Lee, C. Lu and S. J. O'Shea, *Phys. Rev. B: Condens. Matter Mater. Phys.*, 2005, **72**(8), 085405.
74 D. F. Wang, T. Ono and M. Esashi, *Nanotechnology*, 2004, **15**, 1851–1854.
75 J. Tamayo, D. Ramos, J. Mertens and M. Calleja, *Appl. Phys. Lett.*, 2006, **89**(22), 224104.
76 D. Ramos, J. Tamayo, J. Mertens, M. Calleja and A. Zaballos, *J. Appl. Phys.*, 2006, **100**(10), 106105.
77 A. K. Gupta, P. R. Nair, D. Akin, M. R. Ladisch, S. Broyles, M. A. Alam and R. Bashir, *Proc. Natl. Acad. Sci. U. S. A.*, 2006, **103**(36), 13362–13367.
78 B. Ilic, D. Czaplewski, H. G. Craighead, P. Neuzil, C. Campagnolo and C. Batt, *Appl. Phys. Lett.*, 2000, **77**(3), 450–452.
79 M. Zalalutdinov, K. L. Aubin, R. B. Reichenbach, A. T. Zehnder, B. Houston, J. M. Parpia and H. G. Craighead, *Appl. Phys. Lett.*, 2003, **83**(18), 3815–3817.
80 R. B. Reichenbach, M. K. Zalalutdinov, K. L. Aubin, R. Rand, B. H. Houston, J. M. Parpia and H. G. Craighead, *J. Microelectromech. Syst.*, 2005, **14**(6), 1244–1252.
81 S. J. O'Shea, P. Lu, F. Shen, P. Neuzil and Q. X. Zhang, *Nanotechnology*, 2005, **16**, 602–608.
82 S. Evoy, D. W. Carr, L. Sekaric, A. Olkhovets, J. M. Parpia and H. G. Craighead, *J. Appl. Phys.*, 1999, **86**(11), 6072–6077.
83 E. Forsen, G. Abadal, S. Ghatnekar-Nilsson, J. Teva, J. Verd, R. Sandberg, W. Svendsen, F. Perez-Murano, J. Esteve, E. Figueras, F. Campabadal, L. Montelius, N. Barniol and A. Boisen, *Appl. Phys. Lett.*, 2005, **87**(4), 043507.
84 D. Lange, C. Hagleitner, C. Herzog, O. Brand and H. Baltes, *Sens. Actuators, A*, 2003, **103**, 150–155.
85 C. Vančura, J. Lichtenberg, A. Hierlemann and F. Josse, *Appl. Phys. Lett.*, 2005, **87**(16), 162510.
86 D. Jin, J. Lin, X. Li, M. Lin, G. Zuo, Y. Wang, H. Yu and X. Ge, *Proceedings of 1st IEEE International Conference on Nano/Micro Engineered and Molecular Systems*, 2006, Zhuhai, China, p. 832–836.
87 S. Li, L. Orona, Z. Li and Z.-Y. Cheng, *Appl. Phys. Lett.*, 2006, **88**(7), 073507.
88 J. L. Arlett, J. R. Maloney, B. Gudlewski, M. Muluneh and M. L. Roukes, *Nano Lett.*, 2006, **6**(5), 1000–1006.
89 J. Thaysen, A. Boisen, O. Hansen and S. Bouwstra, *Sens. Actuators, A*, 2000, **83**, 47–53.
90 J. H. Lee, K. S. Hwang, J. Park, K. H. Yoon, D. S. Yoon and T. S. Kim, *Biosens. Bioelectron.*, 2005, **20**, 2157–2162.
91 J. W. Yi, W. Y. Shih, R. Mutharasan and W.-H. Shih, *J. Appl. Phys.*, 2003, **93**(1), 619–625.
92 K. S. Hwang, J. H. Lee, J. Park, D. S. Yoon, J. H. Park and T. S. Kim, *Lab Chip*, 2004, **4**, 547.
93 N. V. Lavrik and P. G. Datskos, *Appl. Phys. Lett.*, 2003, **82**(16), 2697–2699.
94 B. Ilic, S. Krylov, K. Aubin, R. Reichenbach and H. G. Craighead, *Appl. Phys. Lett.*, 2005, **86**(19), 193114.
95 M. Zalalutdinov, A. Olkhovets, A. Zehnder, B. Ilic, D. Czaplewski, H. G. Craighead and J. M. Parpia, *Appl. Phys. Lett.*, 2001, **78**(20), 3142–3144.
96 T. E. Schäffer and H. Fuchs, *J. Appl. Phys.*, 2005, **97**(8), 083524.
97 S. Dohn, O. Hansen and A. Boisen, *Appl. Phys. Lett.*, 2006, **88**(26), 264104.
98 L. M. Lechuga, J. Tamayo, M. Álvarez, L. G. Carrascosa, A. Yufera, R. Doldán, E. Peralías, A. Rueda, J. A. Plaza, K. Zinoviev, C. Domínguez, A. Zaballos, M. Moreno, C. Martínez-A, D. Wenn, N. Harris, C. Bringer, V. Bardinal, T. Camps, C. Vergnenègre, C. Fontaine, V. Díaz and A. Bernad, *Sens. Actuators, B*, 2006, **118**, 2–10.
99 X. M. H. Huang, M. Manolidis, S. C. Jun and J. Hone, *Appl. Phys. Lett.*, 2005, **86**(14), 143104.
100 A. Zribi, A. Knobloch and R. Rao, *Appl. Phys. Lett.*, 2005, **86**(20), 203112.

101 Y. Xu, J.-T. Lin, B. W. Alphenaar and R. S. Keynton, *Appl. Phys. Lett.*, 2006, **88**(14), 143513.
102 T. Thundat and L. Maya, *Surf. Sci.*, 1999, **430**, L546–L552.
103 D. Then, A. Vidic and Ch. Ziegler, *Sens. Actuators, B*, 2006, **117**, 1–9.
104 B. Ilic, D. Czaplewski, M. Zalalutdinov, H. G. Craighead, P. Neuzil, C. Campagnolo and C. Batt, *J. Vac. Sci. Technol., B*, 2001, **19**(6), 2825–2828.
105 M. Su, S. Li and V. P. Dravid, *Appl. Phys. Lett.*, 2003, **82**(20), 3562–3564.
106 T. P. Burg and S. R. Manalis, *Appl. Phys. Lett.*, 2003, **83**(13), 2698–2700.
107 L. Johnson, A. K. Gupta, A. Ghafoor, D. Akin and R. Bashir, *Sens. Actuators, B*, 2006, **115**, 189–197.
108 J. S. Bunch, A. M. van der Zande, S. S. Verbridge, I. W. Frank, D. M. Tanenbaum, J. M. Parpia, H. G. Craighead and P. L. McEuen, *Science*, 2007, **315**, 490–493.
109 Y. Wang, J. A. Henry, A. T. Zehnder and M. A. Hines, *J. Phys. Chem. B*, 2003, **107**(51), 14270–14277; J. A. Henry, Y. Wang, D. Sengupta and M. A. Hines, *J. Phys. Chem. B*, 2007, **111**(1), 88–94.
110 J. A. Henry, Y. Wang, D. Sengupta and M. A. Hines, *J. Phys. Chem. B*, 2007, **111**(1), 88.
111 K. L. Ekinci, Y. T. Yang and M. L. Roukes, *J. Appl. Phys.*, 2004, **95**(5), 2682–2689.
112 K. Y. Yasumura, T. D. Stowe, E. M. Chow, T. Pfafman, T. W. Kenny, B. C. Stipe and D. Rugar, *J. Microelectromech. Syst.*, 2000, **9**(1), 117–125.
113 R. Sandberg, K. Mølhave, A. Boisen and W. Svendsen, *J. Micromech. Microeng.*, 2005, **15**, 2249–2253.
114 L. Sekaric, D. W. Carr, S. Evoy, J. M. Parpia and H. G. Craighead, *Sens. Actuators, A*, 2002, **101**, 215–219.
115 K. L. Aubin, M. Zalalutdinov, R. B. Reichenbach, B. H. Houston, A. T. Zehnder, J. M. Parpia and H. G. Craighead, *Proceedings of SPIE, Smart Sensors, Actuators, and MEMS*, 2003, **5116**, Maspalomas, Spain, p. 531–535.
116 T. Alan, M. A. Hines and A. T. Zehnder, *Appl. Phys. Lett.*, 2006, **89**(9), 091901.
117 S. Dohn, R. Sandberg, W. Svendsen and A. Boisen, *Appl. Phys. Lett.*, 2005, **86**(23), 233501.
118 A. R. Kadam, G. P. Nordin and M. A. George, *J. Appl. Phys.*, 2006, **99**(9), 094905.
119 L. B. Sharos, A. Raman, S. Crittenden and R. Reifenberger, *Appl. Phys. Lett.*, 2004, **84**(23), 4638–4640.
120 C. L. Spiel, R. O. Pohl and T. Zehnder Alan, *Rev. Sci. Instrum.*, 2001, **72**(2), 1482–1491.
121 R. N. Kleiman, G. K. Kaminsky, J. D. Reppy, R. Pindak and D. J. Bishop, *Rev. Sci. Instrum.*, 1985, **56**(11), 2088–2091.
122 J. Hessinger and R. O. Pohl, *J. Non-Cryst. Solids*, 1996, **208**, 151–161.
123 X. Liu and R. O. Pohl, *Phys. Rev. B: Condens. Matter Mater. Phys.*, 1998, **58**(14), 9067–9081.
124 M. Spletzer, A. Raman, A. Q. Wu, X. Xu and R. Reifenberger, *Appl. Phys. Lett.*, 2006, **88**(25), 254102.
125 L. A. Bottomley, M. A. Poggi and S. Shen, *Anal. Chem.*, 2004, **76**(19), 5685–5689.
126 S. Basak, A. Raman and S. V. Garimella, *J. Appl. Phys.*, 2006, **99**(11), 114906.
127 T. P. Burg, A. R. Mirza, N. Milovic, C. H. Tsau, G. A. Popescu, J. S. Foster and S. R. Manalis, *J. Microelectromech. Syst.*, 2006, **15**(6), 703–708.
128 T. P. Burg, M. Godin, S. M. Knudsen, W. Shen, G. Carlson, J. S. Foster, K. Babcock and S. R. Manalis, *Nature*, 2007, **446**, 1066.
129 D. Ramos, J. Tamayo, J. Mertens and M. Calleja, *J. Appl. Phys.*, 2006, **99**(12), 124904.
130 T. Braun, V. Barwich, M. K. Ghatkesar, A. H. Bredekamp, C. Gerber, M. Hegner and H. P. Lang, *Phys. Rev. E: Stat. Phys., Plasmas, Fluids, Relat. Interdiscip. Top.*, 2005, **72**(3), 031907.
131 G. G. Yaralioglu, A. Atalar, S. R. Manalis and C. F. Quate, *J. Appl. Phys.*, 1998, **83**(12), 7405–7415.
132 J. Polesel-Maris, L. Aeschimann, A. Meister, R. Ischer, E. Bernard, T. Akiyama, M. Giazzon, P. Niedermann, U. Staufer, R. Pugin, N. F. de Rooij, P. Vettiger and H. Heinzelmann, *J. Phys.: Conf. Ser.*, 2007, **61**, 955–959.
133 X. Yu, J. Thaysen, O. Hansen and A. Boisen, *J. Appl. Phys.*, 2002, **92**(10), 6296–6301.
134 J. A. Harley and T. W. Kenny, *Appl. Phys. Lett.*, 1999, **75**(2), 289–291.